O CZYM PAMIĘTAĆ PODCZAS TWORZENIA MODELI POD DRUK 3D?

IRONCAD | tmsys

POPULARNE TECHNOLOGIE DRUKU 3D

FDM (Fused Deposition Modeling) warstwowe wytłaczanie tworzyw sztucznych

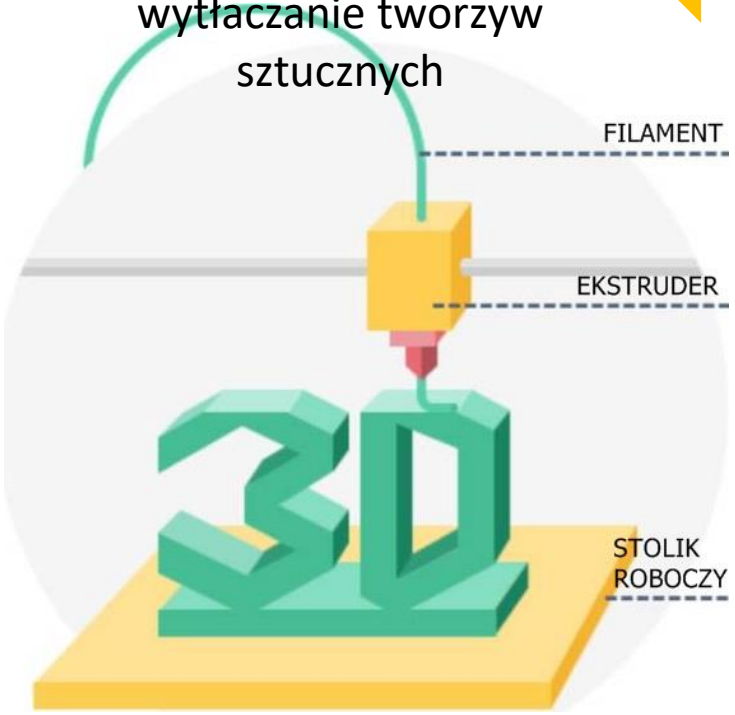

SLA (StereoLithography Apparatus) warstwowe utwardzanie żywic światłoczułych

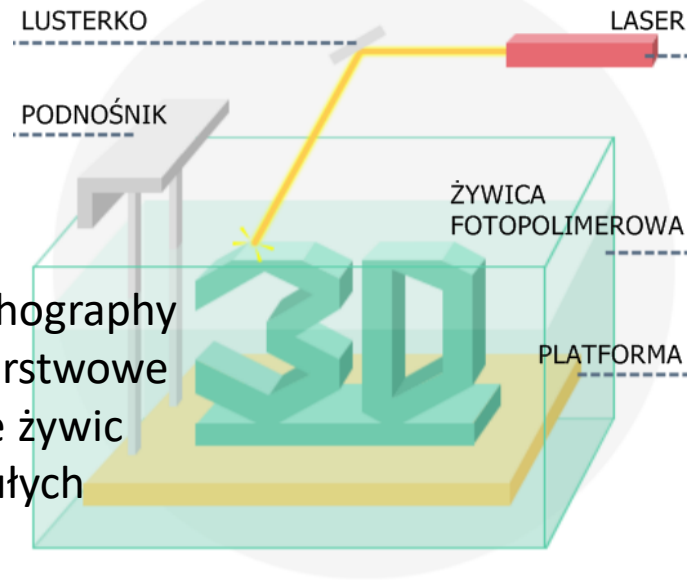

SLS (Selective Laser Sintering) warstwowe laserowe spiekanie proszków polimerowych

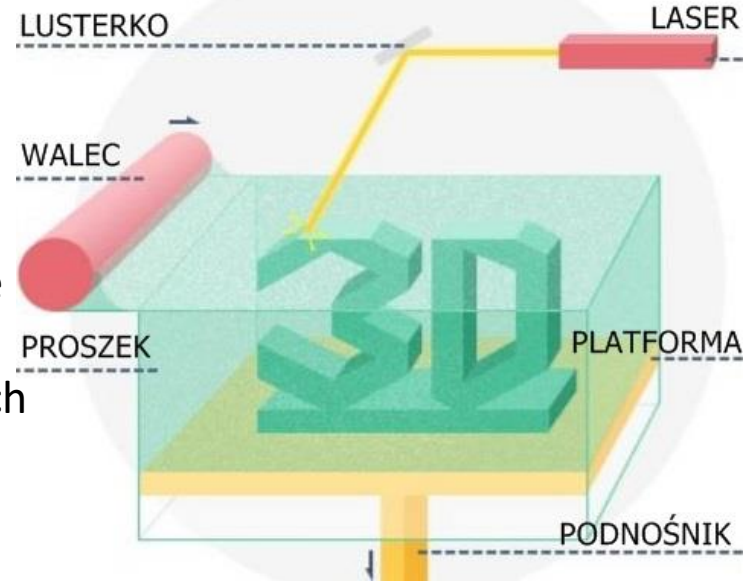

TECHNOLOGIA FDM

FDM polega na warstwowym nakładaniu tworzyw sztucznych wytłaczanych z gorącej dyszy o małej średnicy. Działanie FDM opiera się na selektywnym osadzaniu uplastycznionego tworzywa na platformie roboczej. Materiał w postaci filamentu nagrzewany jest w głowicy do temperatury z zakresu 180°-260°, a następnie wytłaczany na platformę roboczą w postaci cienkiej ścieżki, której szerokość określa średnica robocza dyszy ekstrudera. Ścieżki materiału układane są w pojedyncze warstwy, które łączą się w gotowy model. Technologia ta wymaga stosowania dodatkowych struktur podporowych.

1. Przygotowanie modelu CAD 3D

2. Warstwowe osadzanie tworzywa sztucznego

3. Oczyszczanie struktur wspierających

4. Wysyłka / obróbka dodatkowa modelu

ZASTOSOWANIE TECHNOLOGII FDM

- ✓ Modele koncepcyjne
- ✓ Modele prototypowe
- ✓ Przyrządy i narzędzia produkcyjne
- ✓ Przymiary i wzorniki
- ✓ Elementy konstrukcyjne
- ✓ Mocowania i łączniki
- ✓ Makiety architektoniczne
- ✓ Obudowy urządzeń elektrotechnicznych

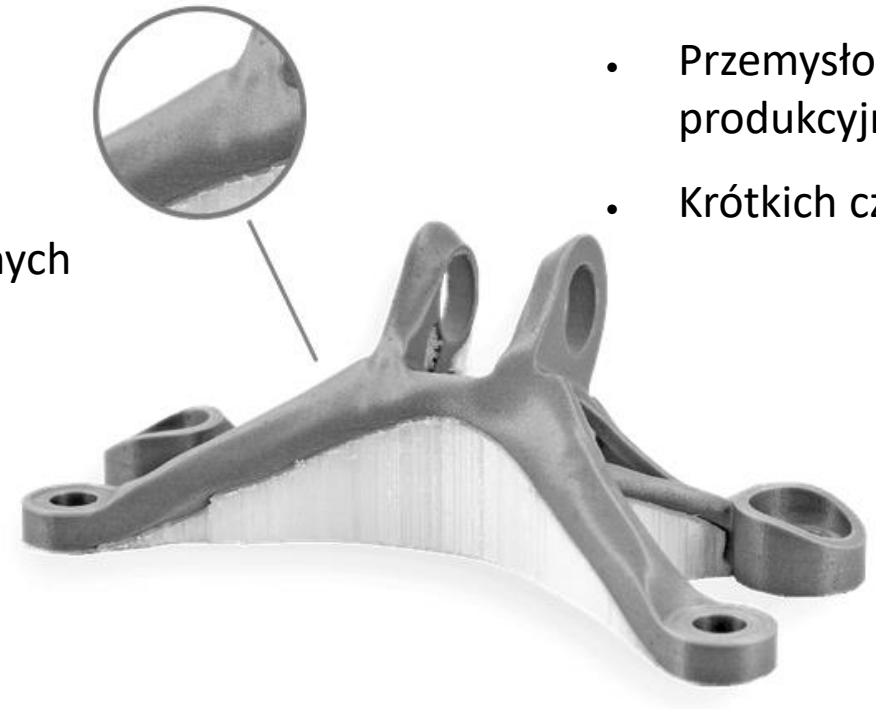

Wybierz FDM, jeśli potrzebujesz…

- Wysokiej dokładności
- Części funkcjonalnych
- Wytrzymałych części
- Przemysłowych materiałów produkcyjnych
- Krótkich czasów realizacji

WYTYCZNE PROJEKTOWE – TECHNOLOGIA FDM

- **MINIMALNA GRUBOŚĆ ŚCIANKI**

  Zalecana wartość: 1.2 mm

  Niewspierana ścianka jest połączona z innymi ściankami mniej niż z dwóch stron. Zaprojektowana mniejsza niż 0,6 mm może ulegać nadmiernemu skurczowi, wypaczaniu lub oderwaniu od modelu podczas drukowania 3D.

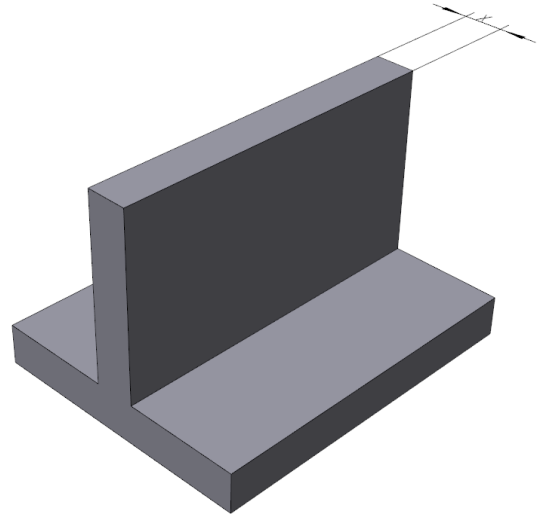

- **MINIMALNA GRUBOŚĆ WSPARTEJ ŚCIANKI**

  Zalecana wartość: 0.8 mm

  Wspierana ścianka jest połączona z dwoma lub więcej innymi ścianami. Geometrie posiadające wartości poniżej zalecanej (0.4 mm) mogą ulegać nadmiernemu skurczowi, wypaczaniu lub oderwaniu od modelu podczas drukowania 3D.

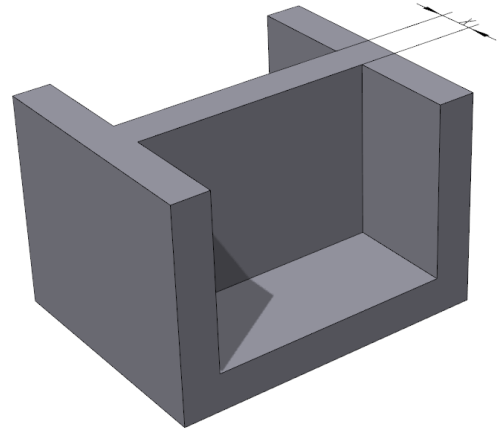

- **MINIMALNY KĄT NAWISU BEZ POTRZEBY WSPIERANIA**

  Zalecana wartość: 40° od poziomu płaszczyzny platformy roboczej

  Minimalny kąt pochylenia dotyczy horyzontalnych i pochylonych ścian. Drukowanie nawisów poniżej zalecanych 40° może ulegać oderwaniu od modelu czy nadmiernemu skurczowi. Negatywny wpływ kąta nawisu w przypadku technologii FDM można minimalizować poprzez odpowiednią orientację modelu w przestrzeni roboczej.

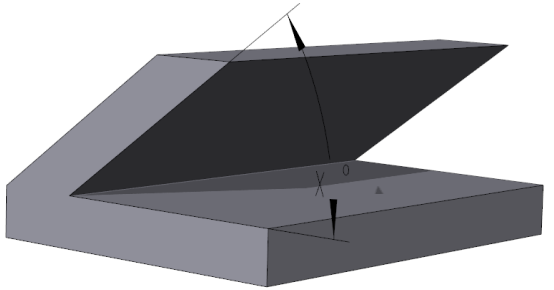

WYTYCZNE PROJEKTOWE – TECHNOLOGIA FDM

- **SZEROKOŚĆ NAWISU BEZ POTRZEBY WSPIERANIA**

  Zalecana wartość: 1 mm

  Nawias odnosi się do geometrii modelu, która horyzontalnie wystaje poza ścianę modelu. Drukowanie nawisów wykraczających poza zalecane parametry może powodować zniekształcenie bądź oderwanie się ww. struktury poza wytwarzany element.

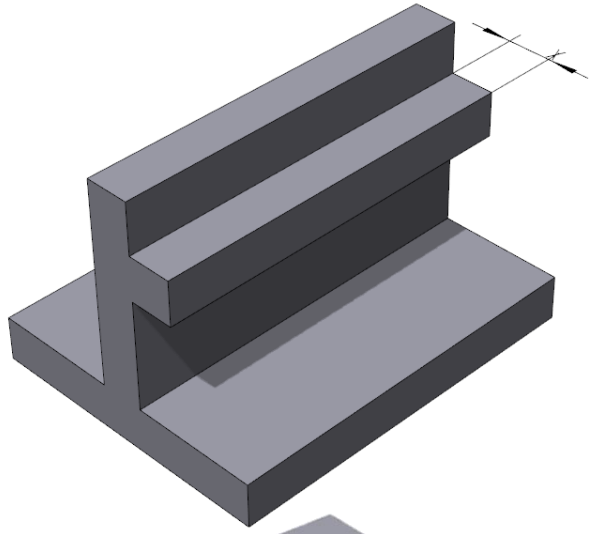

- **MINIMALNA ŚREDNICA OTWORU**

  Zalecana wartość: 2.0 mm

  Otwory zaprojektowane poniżej zalecanej wartości mogą podczas procesu druku 3D ulec zasklepieniu bądź zniekształceniu.

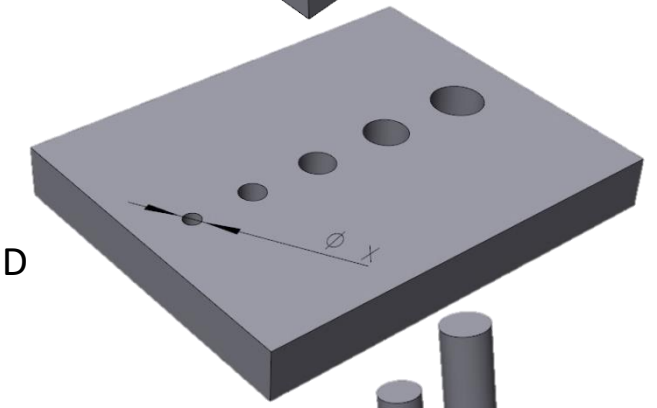

- **MINIMALNA ŚREDNICA WALCA**

  Zalecana wartość: od 1.5 mm (walce niskie) do 5 mm (walce wysokie)

  Podczas projektowania walców o małym przekroju należy pamiętać, że ich właściwości mechaniczne (wytrzymałość) będą stosunkowo niskie.

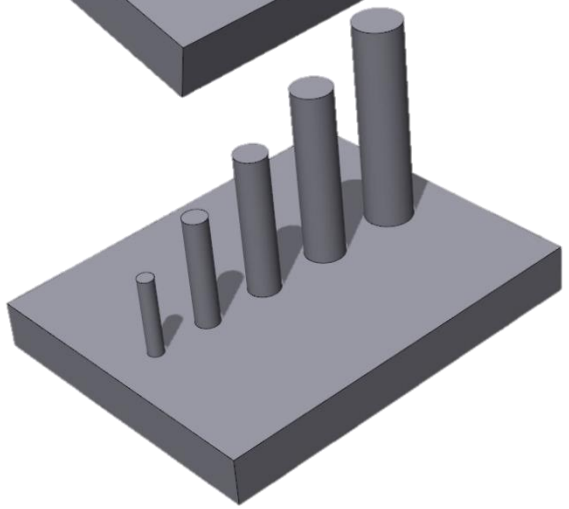

WYTYCZNE PROJEKTOWE – TECHNOLOGIA FDM

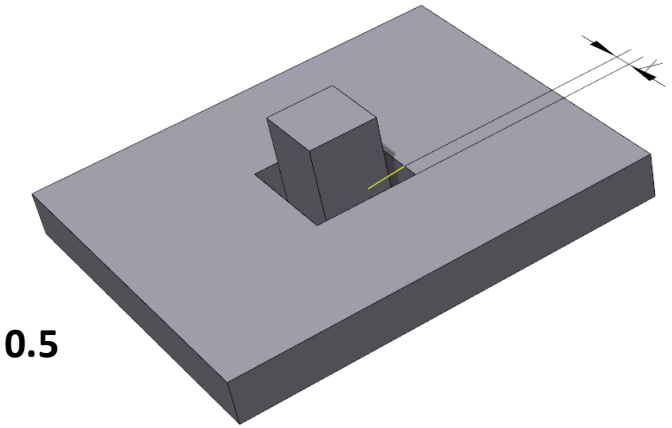

- **MINIMALNY LUZ**

  Zalecana wartość: 0.2 mm (na stronę, elementy przeznaczone złożenia) oraz 0.5 mm (elementy ruchome, podczas druku)

  Luz to odległość będąca różnicą w wymiarach pomiędzy dwoma współpracującymi bądź przeznaczonymi do wzajemnego montażu elementami.

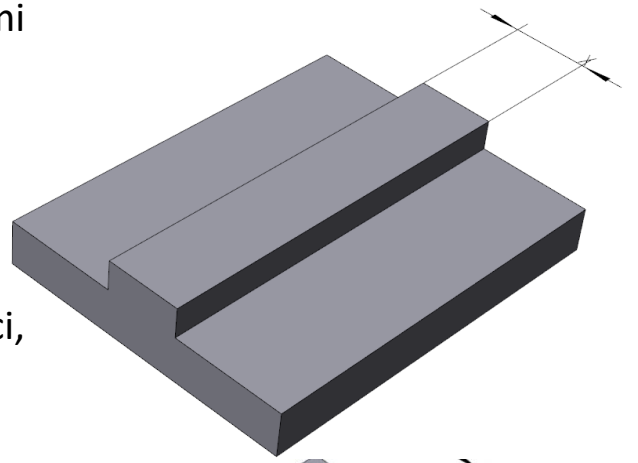

- **MINIMALNY WYCIĄGNIĘTY DETAL**

  Zalecana wartość: 0.3 mm

  Wypukłe szczegóły, takie jak tekst czy tekstura będące poniżej zalecanej wartości, mogą nie być widoczne po procesie druku 3D w technologii FDM.

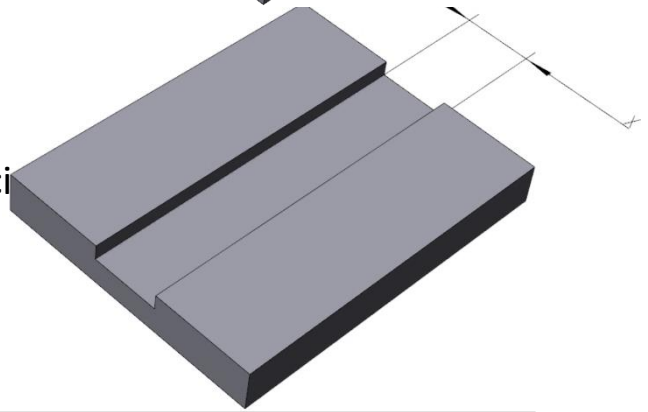

- **MINIMALNY WCIĘTY DETAL**

  Zalecana wartość: 0.4 mm

  Zagłębienia, będące wyciętymi szczegółami znajdujące poniżej zalecanej wartości nie będą widoczne po procesie druku 3D.

TECHNOLOGIA SLS

SLS polega na spajaniu proszków tworzyw sztucznych przy użyciu wiązki lasera. Materiał proszkowy nakładany jest przy użyciu zgarniacza lub rolki na obszar roboczy. Następnie jest podgrzewany i spiekany laserowo. Wiązka laserowa skanuje obszary, które odzwierciedlają aktualny przekrój danego modelu, powodując ich zespolenie. Po spieczeniu laserem danej warstwy, platforma robocza obniża się o grubość warstwy i następuje nałożenie kolejnej porcji materiału. Cykl ten jest powtarzany, aż do uzyskania końcowej geometrii. Nie stosuje się struktur podporowych.

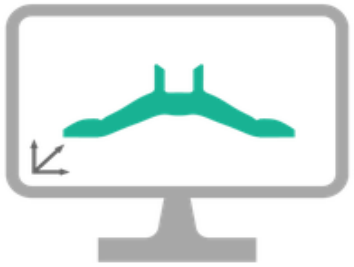

1. Przygotowanie modelu CAD 3D

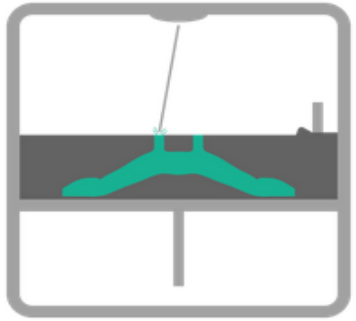

2. Warstwowe spiekanie proszku

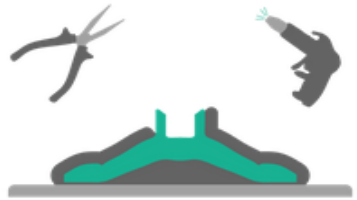

3. Oczyszczanie z luźnego proszku

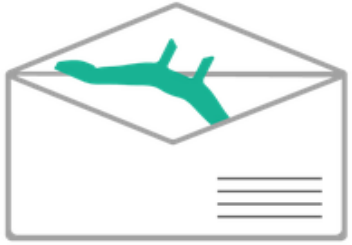

4. Wysyłka / obróbka dodatkowa modelu

ZASTOSOWANIE TECHNOLOGII SLS

- ✓ Modele koncepcyjne i funkcjonalne prototypy
- ✓ Krótkie serie produkcyjne
- ✓ Finalne wyroby
- ✓ Obudowy elektroniki
- ✓ Pomoce warsztatowe
- ✓ Części zamienne i części maszyn
- ✓ Narzędzia pozycjonujące CMM
- ✓ Pomoce warsztatowe
- ✓ Modele architektoniczne, instalacje artystyczne
- ✓ Modele przedoperacyjne i fantomy

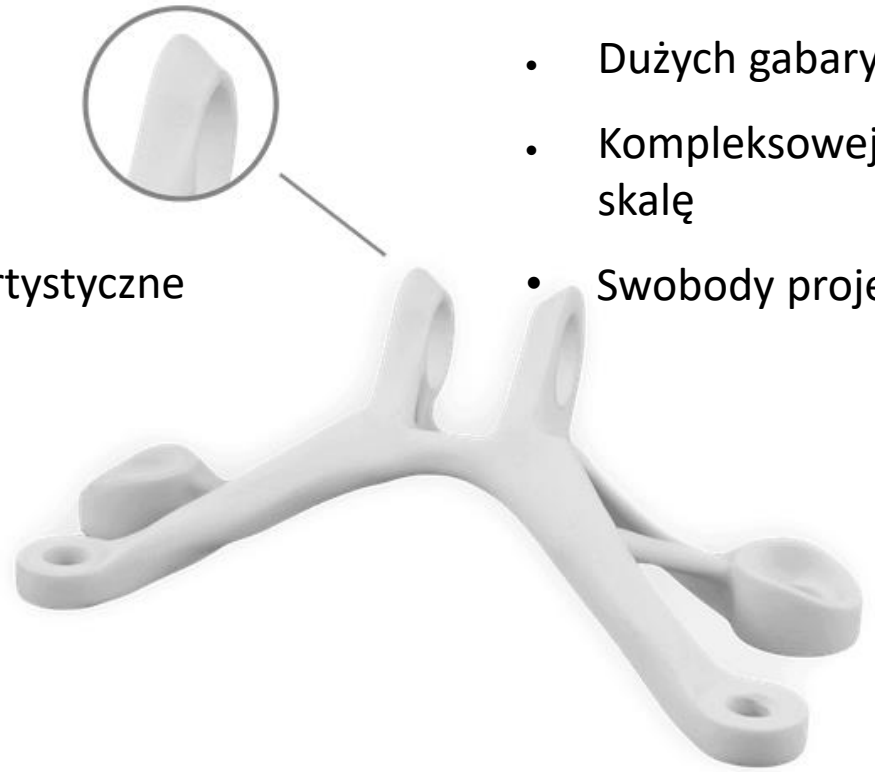

Wybierz SLS, jeśli potrzebujesz…

- Szybkich czasów realizacji i ekonomicznych kosztów
- Wytrzymałych i funkcjonalnych podzespołów
- Dużych gabarytowo i złożonych części
- Kompleksowej produkcji na niewielką skalę
- Swobody projektowania

WYTYCZNE PROJEKTOWE – TECHNOLOGIA SLS

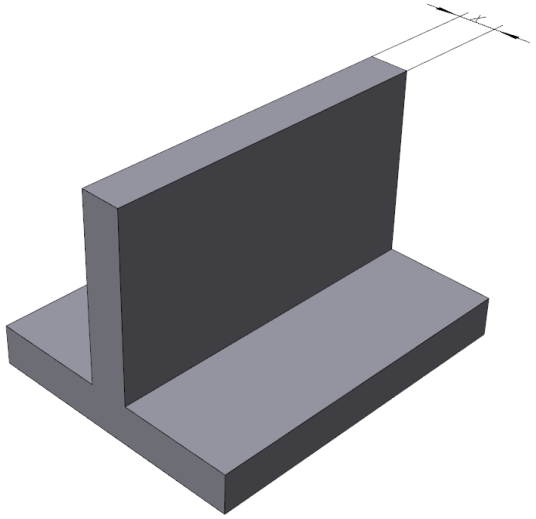

- **MINIMALNA GRUBOŚĆ ŚCIANKI**

  Zalecana wartość: 1.0 mm

  Ścianka niewspierana jest nie połączona z innymi ścianami co najmniej z dwóch stron. Przy zaprojektowanej grubości mniejszej niż 1.0 mm może ulegać nadmiernemu skurczowi, deformacji bądź nie zostać wykryta przez oprogramowania służące do przygotowania procesu.

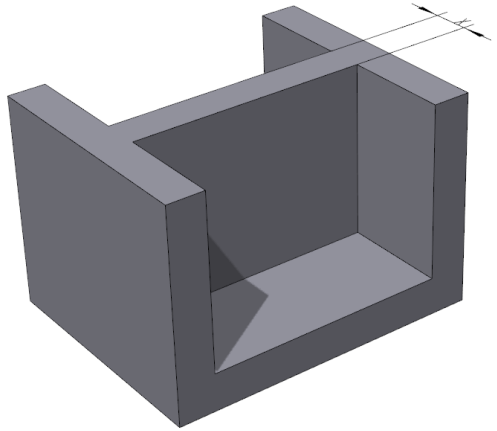

- **MINIMALNA GRUBOŚĆ WSPARTEJ ŚCIANKI**

  Zalecana wartość: 0.8 mm

  Wspierana ścianka jest połączona z dwoma lub więcej innymi ścianami. Geometrie posiadające wartości poniżej zalecanej (0.8 mm) mogą ulegać nadmiernemu skurczowi, deformacji bądź zostać pominięte przez oprogramowania służące do przygotowania procesu.

WYTYCZNE PROJEKTOWE – TECHNOLOGIA SLS

- **MINIMALNA ŚREDNICA OTWORU**

  Zalecana wartość: 0.6 mm

  Otwory zaprojektowane poniżej zalecanej wartości mogą podczas procesu druku 3D ulec zasklepieniu bądź zniekształceniu.

Uwaga! Wartość podana jest dla otworów płytkich, im dłuższy tym wartość minimalna będzie rosnąć.

- **MINIMALNA ŚREDNICA WALCA**

  Zalecana wartość: od 0.8 mm (walce wsparte) do 1.0 mm (walce niewsparte)

  Podczas projektowania walców o małym przekroju należy pamiętać, że ich właściwości mechaniczne (wytrzymałość) będą stosunkowo niskie.

- **MINIMALNY LUZ**

  Zalecana wartość: 0.1 mm (na stronę, elementy przeznaczone do złożenia po procesie) oraz 0.5 mm (elementy ruchome, podczas druku, oddzielane niespieczonym proszkiem)

  Luz to odległość będąca różnicą w wymiarach pomiędzy dwoma współpracującymi bądź przeznaczonymi do wzajemnego montażu elementami.

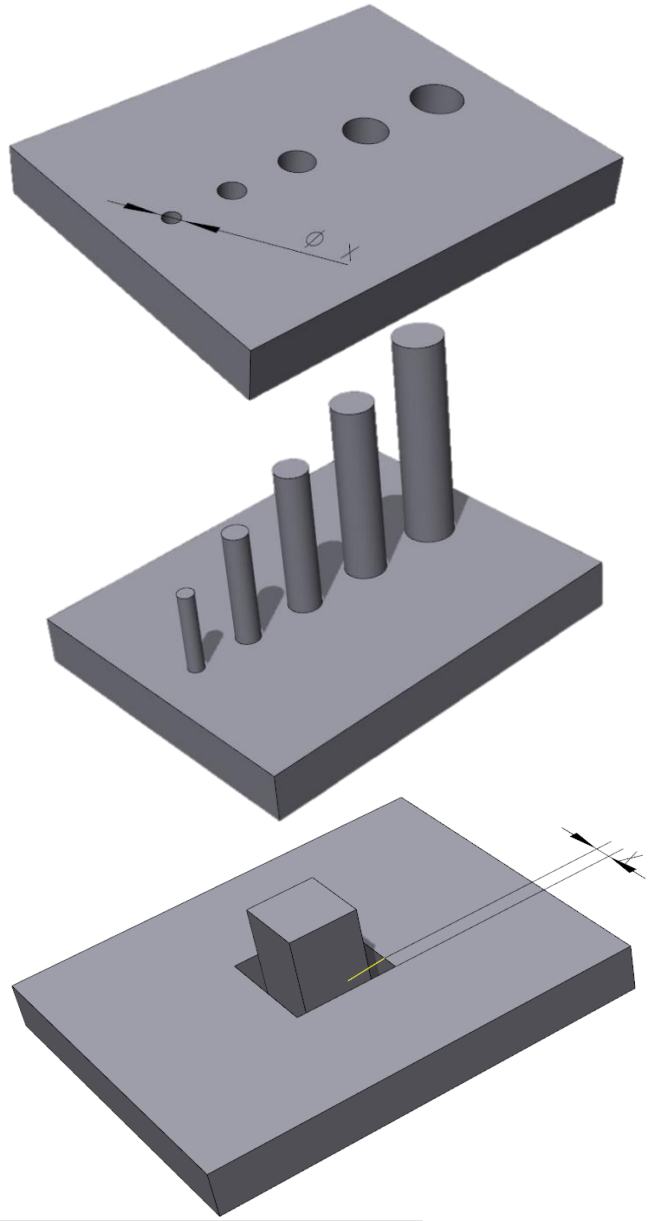

WYTYCZNE PROJEKTOWE – TECHNOLOGIA SLS

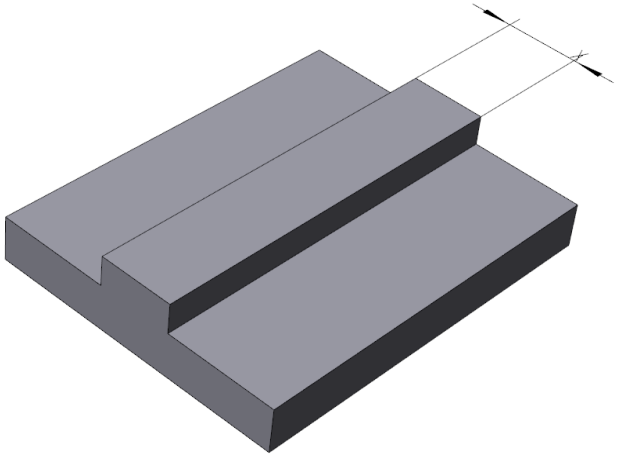

- **MINIMALNY WYCIĄGNIĘTY DETAL**

  Zalecana wartość: 0.5 mm (wysokość), 2.0 mm (szerokość)

  Wypukłe szczegóły (ich wysokość i szerokość), takie jak tekst czy tekstura będące poniżej zalecanej wartości nie będą widoczne po procesie druku 3D w technologii SLS.

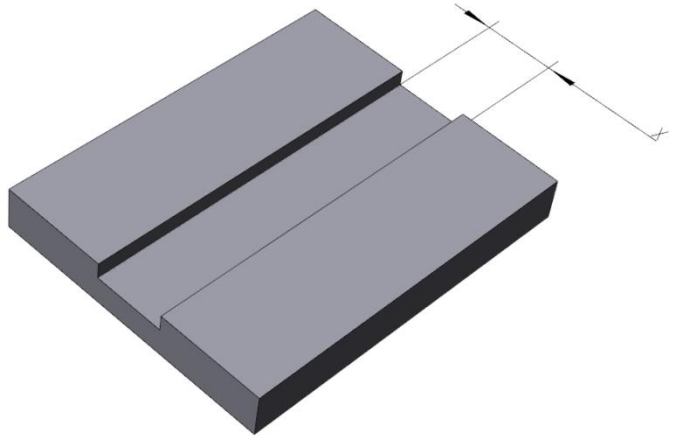

- **MINIMALNY WCIĘTY DETAL**

  Zalecana wartość: 0.5 mm (wysokość), 2.0 mm (szerokość)

  Zagłębienia (ich wysokość i szerokość), będące wyciętymi szczegółami znajdujące poniżej zalecanej wartości nie będą widoczne po procesie druku 3D w technologii SLS.

TECHNOLOGIA SLA

SLA / SL (stereolitografia) polega na utwardzaniu żywicy światłoczułej przy użyciu wiązki lasera, tj. żywicy w której proces polimeryzacji wywoływany jest przy pomocy światła o określonej długości fali. Materiał w formie płynnej żywicy znajduje się w wannie urządzenia. Przed utwardzeniem każdej warstwy zgarniacz przejeżdża przez obszar roboczy, w celu wyrównania tafli cieczy oraz usunięcia z niej pęcherzy powietrza. Ostatnim krokiem jest tzw. skanowanie czyli utwardzanie laserowe. Wiązka laserowa skanuje obszary, odzwierciedlające aktualny przekrój danego modelu, powodując jego polimeryzację (utwardzenie). Następnie platforma robocza obniża się (lub podnosi, w zależności od typu wykorzystywanego urządzenia SLA) o grubość warstwy a opisany cykl powtarza się aż do uzyskania pożądanej i końcowej geometrii.

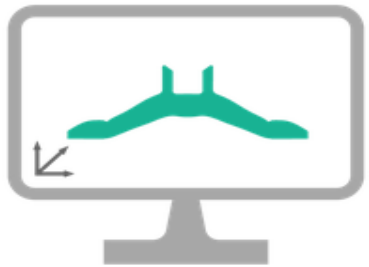

1. Przygotowanie modelu CAD 3D

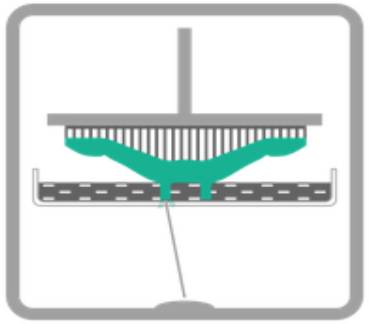

2. Warstwowa fotopolimeryzacja

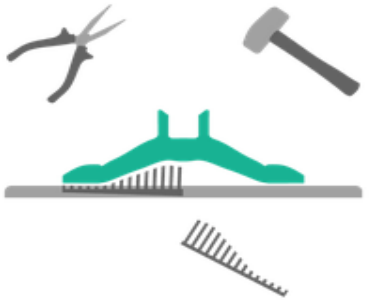

3. Oczyszczanie struktur wspierających

4. Wysyłka / obróbka dodatkowa modelu

ZASTOSOWANIE TECHNOLOGII SLA

- ✓ Modele prototypowe
- ✓ Modele koncepcyjne
- ✓ Modele precyzyjne
- ✓ Modele odlewnicze tracone
- ✓ Elementy konstrukcyjne
- ✓ Modele semi- transparentne
- ✓ Obudowy urządzeń elektrycznych
- ✓ Wzory i przymiary protetyczne

Wybierz SLA, jeśli potrzebujesz…

- Krótkich czasów realizacji, do 24 godzin
- Wysokiego poziomu dokładności oraz jakości powierzchni
- Pokazowych elementów do testów wizualnych
- Dużych pojedynczych części
- Części w pełni transparentnych

WYTYCZNE PROJEKTOWE – TECHNOLOGIA SLA

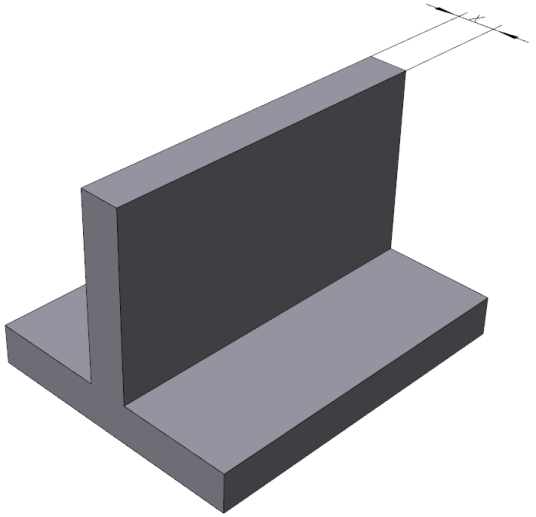

- **MINIMALNA GRUBOŚĆ ŚCIANKI**

  Zalecana wartość: 0.6 mm

  Niewspierana ścianka jest połączona z innymi ściankami mniej niż z dwóch stron. Zaprojektowana mniejsza niż 0,6 mm może ulegać nadmiernemu skurczowi, wypaczaniu lub oderwaniu od modelu podczas drukowania 3D.

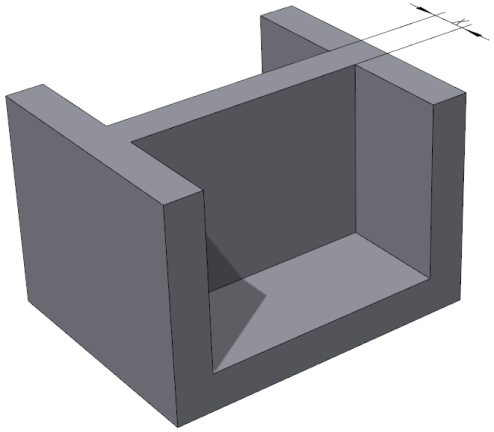

- **MINIMALNA GRUBOŚĆ WSPARTEJ ŚCIANKI**

  Zalecana wartość: 0.4 mm

  Wspierana ścianka jest połączona z przynajmniej dwoma innymi ścianami. Geometrie posiadające wartości poniżej zalecanej (0.4 mm) mogą ulegać nadmiernemu skurczowi, wypaczaniu lub oderwaniu od modelu podczas jego drukowania 3D lub oczyszczania.

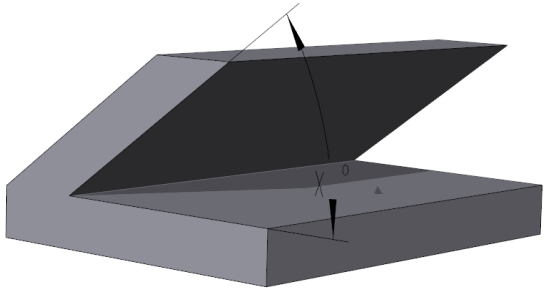

- **MINIMALNY KĄT NAWISU BEZ POTRZEBY WSPIERANIA**

  Zalecana wartość: 19° od poziomu płaszczyzny platformy roboczej

  Minimalny kąt pochylenia dotyczy horyzontalnych i pochylonych ścian. Drukowanie nawisów poniżej zalecanych 19° może spowodować oderwanie tego fragmentu od modelu. Negatywny efekt kąta nawisu w przypadku technologii SLA można minimalizować poprzez odpowiednią orientację modelu w przestrzeni roboczej.

WYTYCZNE PROJEKTOWE – TECHNOLOGIA SLA

- **SZEROKOŚĆ NAWISU BEZ POTRZEBY WSPIERANIA**

  Zalecana wartość: 1 mm

  Nawias odnosi się do geometrii modelu, która horyzontalnie wystaje poza ścianę modelu. Drukowanie nawisów wykraczających poza zalecane parametry może powodować zniekształcenie bądź oderwanie się ww. struktury poza wytwarzany element.

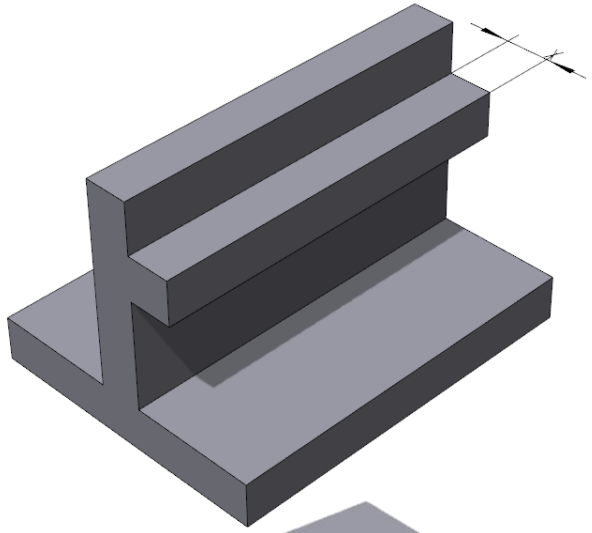

- **MINIMALNA ŚREDNICA OTWORU**

  Zalecana wartość: 0.5 mm

  Otwory zaprojektowane poniżej zalecanej wartości mogą podczas procesu druku 3D ulec zasklepieniu bądź zniekształceniu.

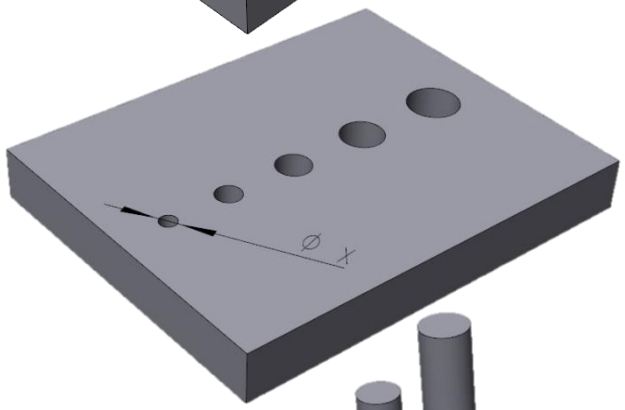

- **MINIMALNA ŚREDNICA WALCA**

  Zalecana wartość: od 0.3 mm (walce niskie) do 1.5 mm (walce wysokie)

  Podczas projektowania walców o małych przekrojach należy pamiętać, że ich właściwości mechaniczne (wytrzymałość) będą stosunkowo niskie.

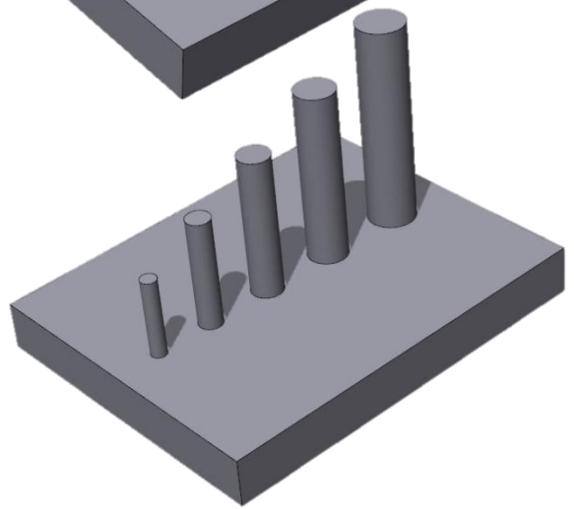

WYTYCZNE PROJEKTOWE – TECHNOLOGIA SLA

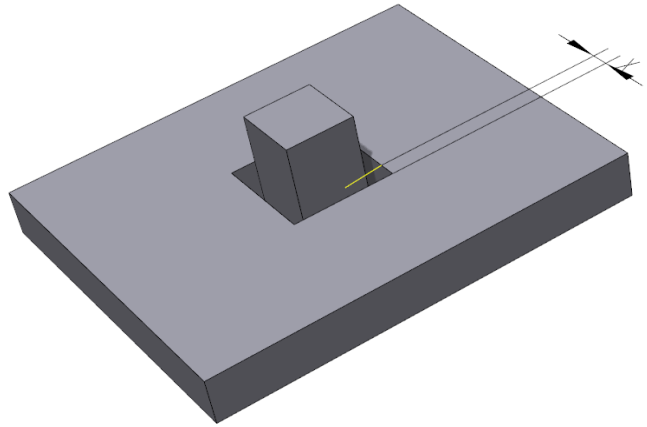

- **MINIMALNY LUZ**

  Zalecana wartość: 0.1 mm (na stronę, elementy przeznaczone złożenia) oraz 0.5 mm (elementy ruchome, podczas druku)

  Luz będący różnicą w wymiarach pomiędzy dwoma współpracującymi bądź przeznaczonymi do wzajemnego montażu elementami.

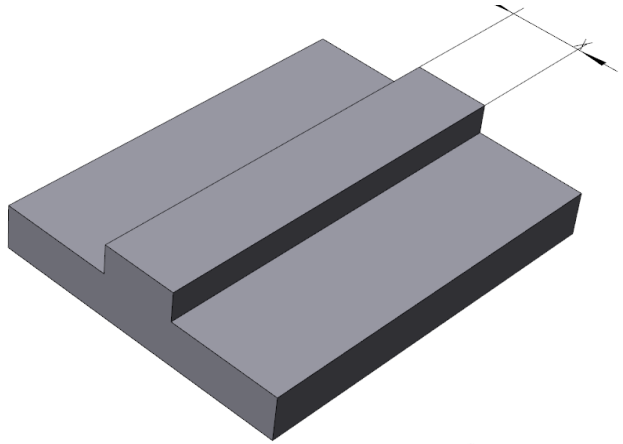

- **MINIMALNY WYCIĄGNIĘTY DETAL**

  Zalecana wartość: 0.1 mm

  Wypukłe szczegóły, takie jak tekst czy tekstura będące poniżej zalecanej wartości nie będą widoczne po procesie druku 3D w technologii SLA.

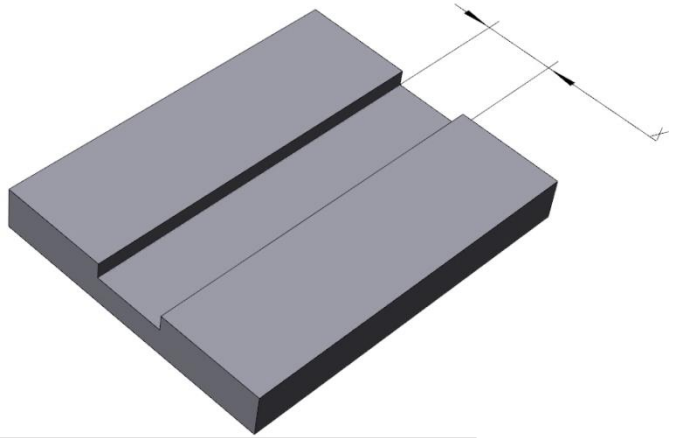

- **MINIMALNY WCIĘTY DETAL**

  Zalecana wartość: 0.4 mm

  Zagłębienia, będące wyciętymi szczegółami znajdujące poniżej zalecanej wartości nie będą widoczne po procesie druku 3D.

TWORZENIE MODELI W CAD 3D

Wykorzystanie modelu CAD 3D zapewnia:

- Zwiększenie wydajności i niezawodności
- Automatyczne wprowadzanie zmian
- Oszczędność czasu i pieniędzy
- Zarządzanie projektem

W programie **IRONCAD CAD 3D** istnieje możliwość tworzenia modeli pod druk 3D. Projekt możemy zapisać w **formacie .STL** wybierając odpowiednie ustawienia eksportu.

Modele w formacie .STL są bryłami, których powierzchnie składają się z trójkątów. Zaleca się aby wybrać w ustawieniach powierzchnię **o wartości 240**.

Przed wydrukiem warto sprawdzić wyeksportowany plik w darmowym programie dla druku 3D czy nie zawiera on błędów.

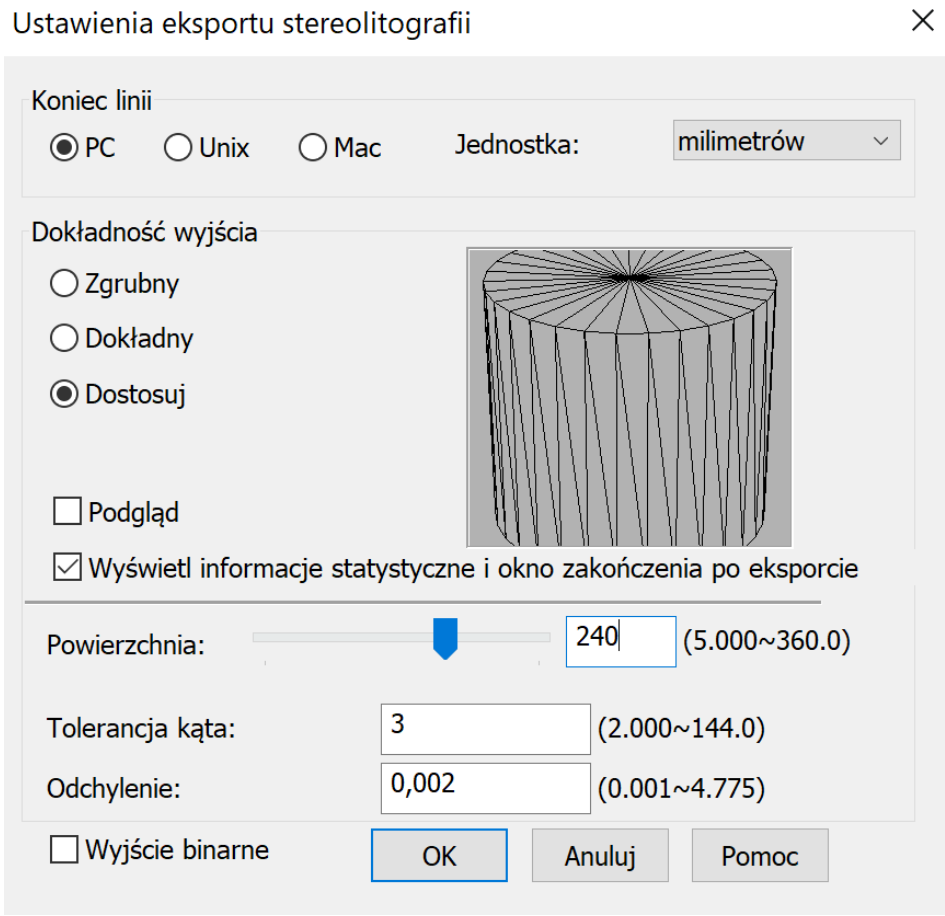

PODSUMOWANIE -projektuj świadomie!

- W przypadku uzasadnionego, ekonomicznego podejścia do wykonania obiektu fizycznego przy pomocy druku 3D, należy pamiętać o cechach i powierzchniach obiektu, na których najbardziej nam zależy.

- Orientacja obiektu w komorze roboczej urządzenia definiuje powierzchnie i detale wymagające dodatkowego wsparcia. Nie zawsze da się obrócić model tak, aby go uniknąć. Warto zwrócić na to uwagę już na etapie projektowania, ponieważ często można zminimalizować ilość wspieranych powierzchni, nie ujmując funkcjonalności projektowanego elementu a poprawiając jakość otrzymanego detalu.

- Projektując daną geometrię, należy pamiętać o ograniczeniach związanych z technologią wytwarzania. Jest to ważna kwestia w sytuacji, w której projektowane obiekty mają być wykonywane w małych seriach wykorzystując technologie przyrostowe.

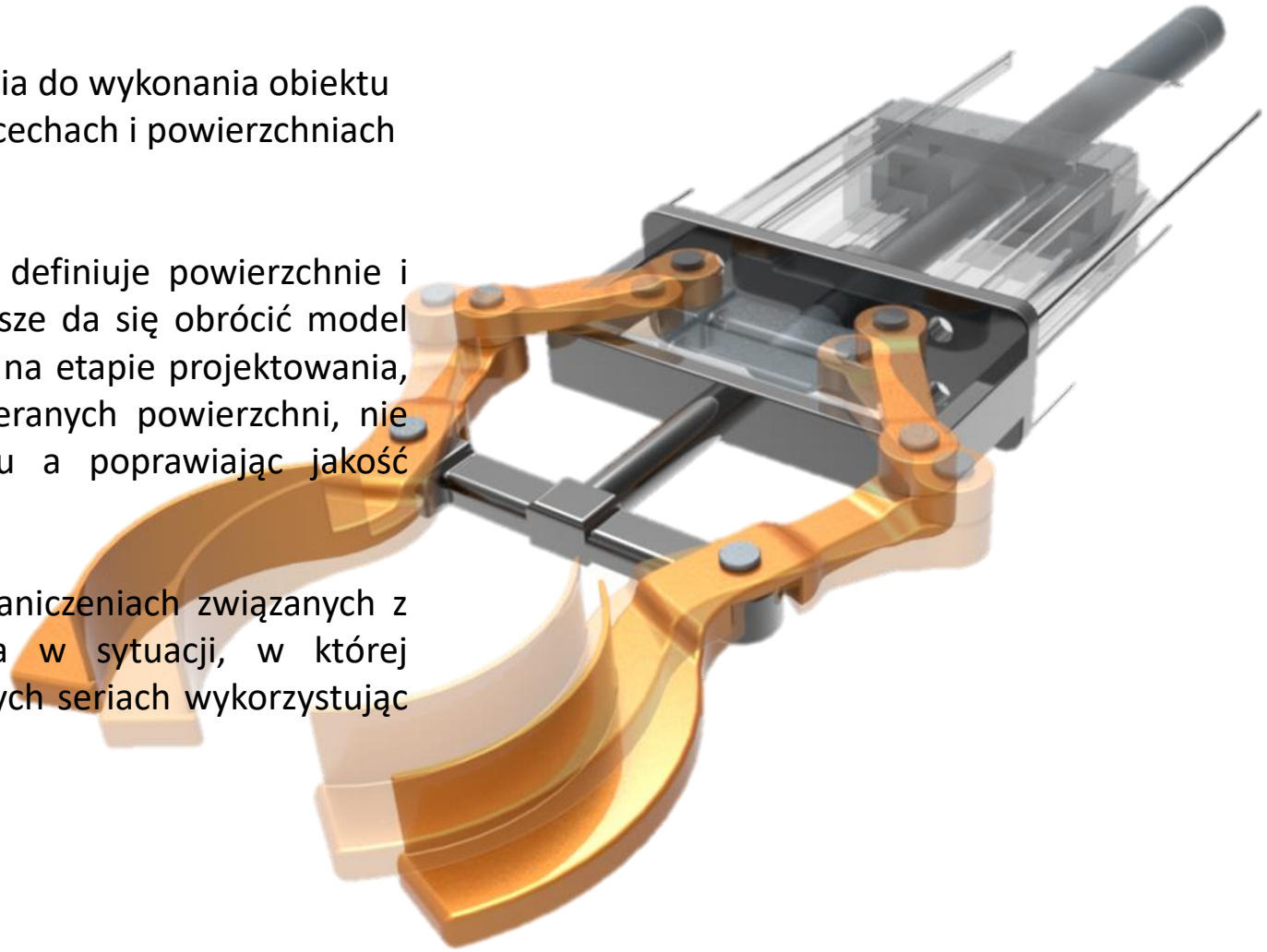

ZAKOŃCZENIE

W powyższym poradniku zawarliśmy przykładowe wytyczne podczas tworzenia modeli do druku 3D w 3 wybranych technologiach: FDM, SLS, SLA .

Chcesz dowiedzieć się więcej o programie IRONCAD CAD 3D ? Jesteś zainteresowany poznaniem technologii druku 3D?

Umów się z nami na bezpłatną i niezobowiązującą prezentację programu. Nasi specjaliści chętnie pokażą funkcjonalność i możliwości programu IRONCAD CAD 3D oraz doradzą w wyborze sprzętu do druku 3D.

SKONTAKTUJ SIĘ Z NAMI:

TMSys Sp. z o.o.
ul. Ciepłownicza 23
31-574 Kraków

e-mail: info@ironcad.pl
tel.: 12 362 30 76

Oddział Północ
ul. Abrahama 6
84-300 Lębork

e-mail: polnoc@ironcad.pl
tel.: 59 333 00 95

Chapter 7
Compliant Mechanisms

Larry L. Howell

7.1 Introduction

Compliant mechanisms[1] gain their motion from the deflection of elastic members. Examples of compliant mechanisms are shown in Fig. 7.1. Because compliant mechanisms gain their motion from the constrained bending of flexible parts, they can achieve complex motion from simple topologies. Traditional mechanisms use rigid parts connected at articulating joints (such as hinges, axles, or bearings), which usually requires assembly of components and results in friction at the connecting surfaces [21, 31, 46]. Because traditional bearings are not practical in many situations (e.g. microelectro-mechanical systems) and lubrication can be problematic, friction and wear present major difficulties. Compliant mechanisms also offer an opportunity to achieve complex motions within the limitations of micro- and nano-fabrication.

Nature provides an example of how to effectively create controlled motion. Most moving components in nature are flexible instead of stiff, and the motion comes from bending the flexible parts instead of rigid parts connected with hinges (for example, consider hearts, elephant trunks, and bee wings). The smaller the specimen, the more likely it is to use the deflection of flexible components to obtain its motion [21].

7.1.1 Advantages of Compliant Mechanisms

Some of the advantages of compliant mechanisms include the following:

[1]This section is based on "Compliant Mechanisms" by L.L. Howell in *Encyclopedia of Nanotechnology*, Editor: B. Bhusham, © Springer, 2012, used with permission.

L.L. Howell (✉)
Brigham Young University, Provo, UT, USA
e-mail: lhowell@byu.edu

J.M. McCarthy (ed.), *21st Century Kinematics*,
DOI 10.1007/978-1-4471-4510-3_7, © Springer-Verlag London 2013

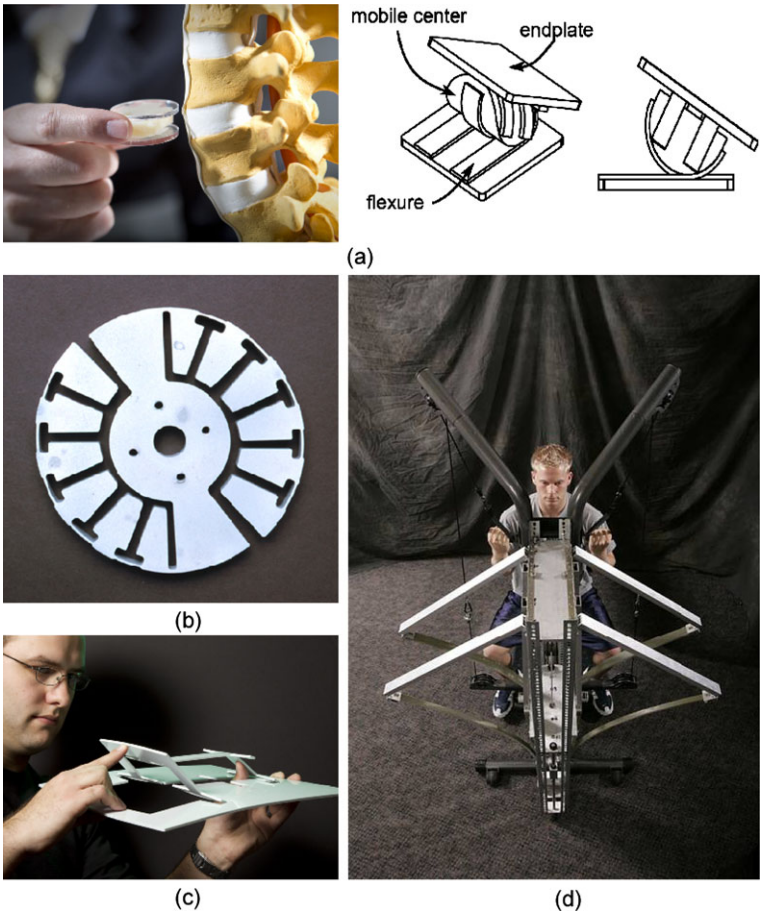

Fig. 7.1 Example compliant mechanisms. (**a**) An artificial spinal disc. (**b**) A compliant centrifugal clutch. (**c**) A lamina emergent mechanism. (**d**) A compliant constant-force exercise machine

Can Be Made From One Layer of Material Compliant mechanisms can be fabricated from a single layer. This makes them compatible with many common microelectromechanical system (MEMS) fabrication methods, such as surface micromachining, bulk micromachining, and LIGA. For example, consider the folded beam suspension shown in Fig. 7.2. This device is often used as a suspension element in MEMS systems. It offers a simple approach for constrained linear motion, and also integrates a return spring function. The device can achieve large deflections with reasonable off-axis stiffness. The compliant mechanism makes it possible to do these functions with a single layer of material.

No Assembly Required Compliant mechanisms that gain all of their motion from the deflection of flexible components are "fully compliant mechanisms," where devices that combine both traditional and compliant elements are called "partially

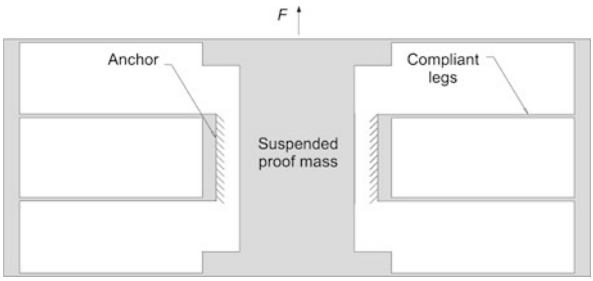

Fig. 7.2 A folded-beam suspension is an example of a widely used compliant mechanism in microelectromechanical systems (MEMS) applications

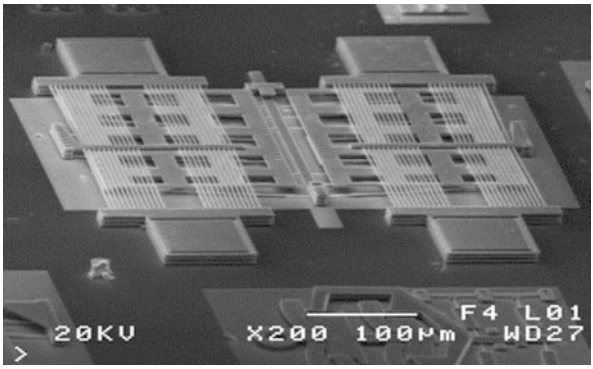

Fig. 7.3 This scanning electron micrograph shows a thermal actuator that uses multiple layers of compliant elements to achieve large amplification with a small footprint

compliant mechanisms". Fully compliant mechanism can usually be fabricated without assembly of different components.

Compact Some compliant mechanisms can also be designed to have a small footprint. Various strategies can be used to decrease the size of a mechanism. Figure 7.3 shows a thermal actuator that uses multiple layers to achieve a small footprint.

Friction-Free Motion Because compliant mechanisms gain their motion from deflection of flexible members rather than from traditional articulating joints, it is possible to reduce or eliminate the friction associated with rubbing surfaces. This results in reduced wear and eliminates the need for lubrication, as described next.

Wear-Free Motion Wear can be particularly problematic in biomedical applications, precision mechanisms, and at small scales. The elimination of friction can result in the elimination of wear at the connecting surfaces of joints. For devices that are intended to undergo many cycles of motion, eliminating friction can dramatically increase the life of the system.

No Need for Lubrication Another consequence of eliminating friction is that lubricants are not needed for the motion. This is particularly important in biomedical implants, space applications, and at small scales where lubrication can be problematic.

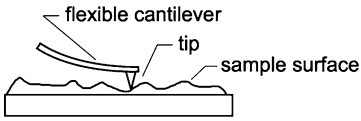

Fig. 7.4 The cantilever of an atomic force microscope (AFM) is an example of compliance employed in high precision instruments

High Precision Flexures have long been used in high precision instruments because of the repeatability of their motion. Some reasons for compliant mechanisms precision are the backlash-free motion inherent in compliant mechanisms and the wear-free and friction-free motion described above. The cantilever associated with an atomic force microscope (Fig. 7.4) is an example application.

Integrated Functions Like similar systems in nature, compliant mechanisms have the ability to integrate multiple functions into few components. For example, compliant mechanisms often provide both the motion function and a return-spring function. Thermal actuators are another example of integration of functions, as described later.

High Reliability The combination of highly constrained motion of compliant mechanisms and wear-free motion result in high reliability of compliant mechanisms.

7.1.2 Challenges of Compliant Mechanisms

Compliant mechanisms have many advantages, but they also have some significant challenges. A few of these are discussed below [21]:

Limited Rotation One drawback of compliant mechanisms is that most are unable to undergo continuous rotation. Also, if a fully compliant mechanism is constructed from a single layer of material, then special care has to be taken to ensure that moving segments of the compliant mechanism do not collide with other segments of the same mechanism.

Dependence on Material Properties The performance of compliant mechanisms is highly dependent on the material properties, which are not always well known.

Nonlinear Motions The deflections experienced by compliant mechanisms of-ten extend beyond the range of linearized beam equations. This can make their analysis and design more complicated.

Fatigue Analysis Because most compliant mechanisms undergo repeated loading, it is important to consider the fatigue life of the device. An understanding of how to achieve controlled compliant mechanism motion and the associated stresses,

makes it possible to design compliant mechanisms with the desired fatigue life. Interestingly, because of the types of materials used and their purity, many MEMS compliant mechanisms will either fail on their first loading cycle or will have infinite fatigue life. Because of the low inertia of MEMS devices, it is often easy to quickly test a MEMS device to many millions of cycles. Factors such as stress concentrations, the operating temperature, and other environment conditions can affect the fatigue life.

Difficult Design Integration of functions into fewer components, nonlinear displacements, dependence on material properties, the need to avoid self collisions during motion, and designing for appropriate fatigue life, all combine to make the design of compliant mechanisms nontrivial and often difficult.

7.1.3 Analysis and Design of Compliant Mechanisms

Multiple approaches are available for the analysis and design of compliant mechanisms. Three of the most developed approaches are described below.

7.1.3.1 Finite Element Analysis

Finite element methods are the most powerful and general methods available to analyze compliant mechanisms. Commercial software is currently available that has the capability of analyzing the large, nonlinear deflections often associated with compliant mechanisms. The general nature of the method makes it applicable for a wide range of geometries, materials, and applications. Increasingly powerful computational hardware has made it possible to analyze even very complex compliant mechanisms. It is also possible to use finite element methods in the design of compliant mechanisms, particularly once a preliminary design has been determined. But in the early phases of design, other methods (or hybrid methods) are often preferred so that many design iterations can be quickly analyzed.

7.1.3.2 Topology Optimization

Suppose that all that is known about a design is the desired performance and design domain. Topology optimization shows promise for designing compliant mechanisms under such conditions. The advantage is that very little prior knowledge about the resulting compliant mechanism is needed, and any biases of the designer are eliminated [10]. Topology optimization is often integrated with finite element methods to consider many possible ways of distributing material with the design domain. This has the potential to find designs that would not otherwise be discovered by other methods. Infinite possible topologies are possible and finite element

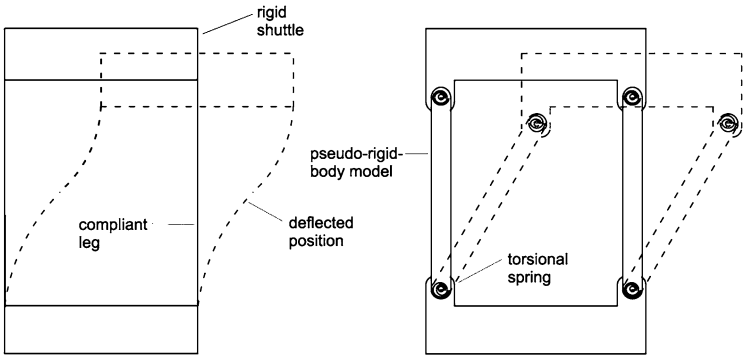

Fig. 7.5 The pseudo-rigid-body model of the compliant parallel-guiding mechanism consists of appropriately located pin joints and torsional springs. (This device is a building block of other devices, such as the folded-beam suspension)

methods can be employed to evaluate the different possibilities. The resolution of the design domain mesh can be a limiting factor, but once a desirable topology is identified, it can be further refined using other approaches.

7.1.3.3 Pseudo-Rigid-Body Model

The pseudo-rigid-body model is used to model compliant mechanisms as traditional rigid-body mechanisms, which opens up the possibility of using the design and analysis methods developed for rigid-body mechanisms in the design of compliant mechanisms [10]. With the pseudo-rigid-body model approach, flexible parts are modeled as rigid links connected at appropriately placed pins, with springs to represent the compliant mechanisms resistance to motion. Extensive work has been done to develop pseudo-rigid-body models for a wide range of geometries and loading conditions. Consider a simple example. The mechanism shown in Fig. 7.5 has a rigid shuttle that is guided by two flexible legs. (Note that the folded-beam suspension in Fig. 7.2 has four of these devices connected in series and parallel.) The pseudo-rigid-body model of the mechanism models the flexible legs as rigid links connected at pin joints with torsional springs. Using appropriately located joints and appropriately sized springs, this model is very accurate well into the nonlinear range. For example, if the flexible legs are single walled carbon nanotubes, comparisons to molecular simulations have shown the pseudo-rigid-body model to provide accurate results [18]. The advantages of the pseudo-rigid-body model are realized during the early phases of design where many design iterations can be quickly evaluated, traditional mechanism design approaches can be employed, and motions can be easily visualized.

The pseudo-rigid-body model approach is described in more detail in the following section. When the configuration of a compliant device is already known, nonlinear finite element analysis may be used to analyze its behavior. However, if instead

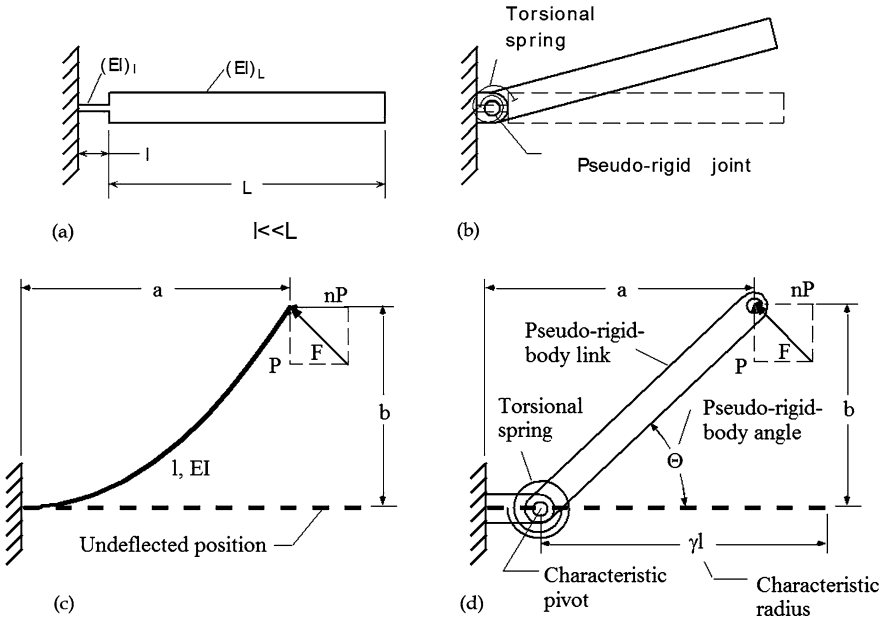

Fig. 7.6 Examples of flexible segments and their pseudo-rigid-body models. (**a**) A small-length flexural pivot, (**b**) its pseudo-rigid-body model, (**c**) a fixed-pinned segment, (**d**) its pseudo-rigid-body model

of knowing the device configuration, all that is known is the task that must be performed and the configuration and dimensions must be synthesized, then nonlinear finite element analysis alone is not a realistic approach because of the many iterations and computation required. Recently, the pseudo-rigid-body model has been developed for the analysis and design of compliant mechanisms. The pseudo-rigid-body model concept analyzes large-deflection beams as rigid links with appropriately placed pin joints and torsional springs. The result is that an otherwise complicated compliant mechanism may be modeled as a rigid-link mechanism. This unification of compliant mechanism theory and traditional rigid-link mechanism theory allows the vast amount of knowledge available for the design of rigid-link mechanisms to be applied to compliant mechanisms.

Individual Flexible Segments Pseudo-rigid-body models have been developed for various types of compliant segments, two of which will be reviewed here.

Small-Length Flexural Pivots [20] The simplest segment is the small-length flexural pivot. Consider a flexible segment that has a much smaller length than the more rigid section, as illustrated in Fig. 7.6(a). The motion of the end of the beam is due to elastic deflection of the flexible segment, which is amplified by the rigid-body rotation of the rigid segment. This motion can be modeled by a pin joint located at the center of the flexible segment, as shown in Fig. 7.6(b). The resistance to motion

is modeled by a torsional spring. The length of the pseudo-rigid link, r, is

$$r = L + \frac{l}{2}, \tag{7.1}$$

where l is the length of the flexible segment and L is the length of the rigid segment. The value of the torsional spring constant, K, is

$$K = \frac{EI}{l}, \tag{7.2}$$

where E is the Youngs modulus, and I is the area moment of inertia. This model is quite accurate for large deflections for cases where L is much greater than l.

Fixed-Pinned Segment [19] A long, flexible, cantilever beam with a force at the free end is shown in Fig. 7.6(c). The end of the beam follows a path that is very nearly circular for a very large deflection. This implies that the deflection can be accurately modeled by two rigid links pinned at the center of the circular path. Figure 7.6(d) shows the pseudo-rigid-body model for the beam. The location of the characteristic pivot is defined by the nondimensional "characteristic radius factor," γ. The length of the pseudo-rigid link, r, is

$$r = \gamma l. \tag{7.3}$$

The resistance to deflection is modeled by a torsional spring with a torsional spring constant, K, of

$$K = \gamma K_\Theta \frac{EI}{l}. \tag{7.4}$$

The deflections of the beam are now easily calculated. The vertical deflection, b, is

$$b = \gamma l \sin \Theta, \tag{7.5}$$

where Θ is the angle of the pseudo-rigid-link. The horizontal deflection, a, is

$$a = l(1 - \gamma) \cos \Theta. \tag{7.6}$$

Typical values of K_γ and Θ are 0.85 and 2.65, respectively. The boundary conditions for the fixed-pinned beam described earlier are one end fixed (force and moment reactions), and the other end pinned (force reactions only).

Other Segments Pseudo-rigid-body models have been developed for other types of segments, including fixed-guided segments, functionally binary pinned-pinned segments, beams loaded with a moment at the end, and beams with follower loads.

Mechanisms. The real power of the pseudo-rigid-body model for individual segments is realized when they are applied to compliant mechanisms that contain such elements. For example, consider the compliant bistable mechanism illustrated in

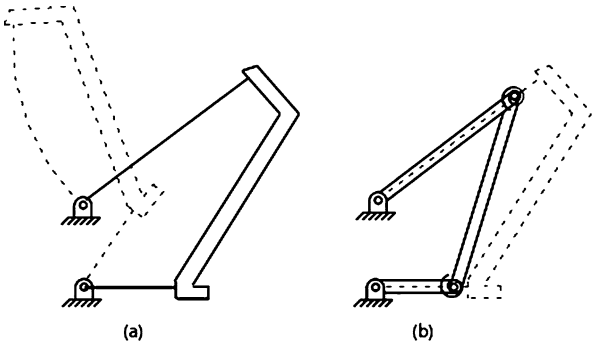

Fig. 7.7 (**a**) A bistable compliant mechanism and (**b**) its pseudo-rigid-body model

Fig. 7.7(a). Since the flexible segments have the geometry and boundary conditions of the fixed-pinned segment discussed earlier, they can be modeled using the pseudo-rigid-body model for that segment. The resulting pseudo-rigid-body model for the mechanism is shown in Fig. 7.7(b). This mechanism will be discussed in more detail as an example.

Example model. Consider a brief example for the compliant, micro, bistable mechanism illustrated in Fig. 7.7(a) [29]. Its corresponding pseudo-rigid-body model is shown in Fig. 7.7(b). The torsional spring constants are calculated from the geometry and material properties. The potential energy, V, for the mechanism is

$$V = \frac{1}{2}(K_2\psi_2 + K_3\psi_3), \tag{7.7}$$

where K_i is the spring constant for joint i, and

$$\psi_2 = (\theta_2 - \theta_{20}) - (\theta_3 - \theta_{30}) \quad \text{and} \quad \psi_3 = (\theta_4 - \theta_{40}) - (\theta_3 - \theta_{30}) \tag{7.8}$$

and θ_i is the angle of link i, which can be found using traditional kinematic analysis. The input torque, M_2, is

$$M_2 = \frac{dV}{d\theta_2} = K_2\psi_2(1 - h_{32}) + K_3\psi_3(h_{42} - h_{32}), \tag{7.9}$$

where

$$h_{32} = \frac{r_2\sin(\theta_4 - \theta_2)}{r_3\sin(\theta_3 - \theta_4)} \quad \text{and} \quad h_{42} = \frac{r_2\sin(\theta_3 - \theta_2)}{r_4\sin(\theta_4 - \theta_3)}. \tag{7.10}$$

The second derivative of the potential energy (the stiffness) is

$$\begin{aligned}\frac{d^2V}{d\theta_2^2} &= K_2\left(1 - 2h_{32} + h_{32}^2 - \psi_2 h'_{32}\right) \\ &\quad + K_3\left[h_{42}^2 - 2h_{42}h_{32} + h_{32}^2 + \psi_3\left(h'_{42} - h'_{23}\right)\right],\end{aligned} \tag{7.11}$$

where

$$h'_{32} = \frac{dh_{32}}{d\theta_2} = \frac{r_2}{r_3}\left[\frac{\cos(\theta_4 - \theta_2)}{\sin(\theta_3 - \theta_4)}(h_{42} - 1) - \frac{\sin(\theta_4 - \theta_2)\cos(\theta_3 - \theta_4)}{\sin^2(\theta_3 - \theta_4)}(h_{32} - h_{42})\right], \tag{7.12}$$

$$h'_{42} = \frac{dh_{42}}{d\theta_2} = \frac{r_2}{r_4}\left[\frac{\cos(\theta_3 - \theta_2)}{\sin(\theta_3 - \theta_4)}(h_{32} - 1) - \frac{\sin(\theta_3 - \theta_2)\cos(\theta_3 - \theta_4)}{\sin^2(\theta_3 - \theta_4)}(h_{32} - h_{42})\right]. \tag{7.13}$$

The potential energy curve (equation (7.9)), the required crank torque (equation (7.11)), and the second derivative of potential energy (equation (7.13)) are particularly useful in defining the mechanism behavior. The input torque is zero at points of relative minimum (stable equilibrium position) or maximum (unstable equilibrium) potential energy. The global minimum of potential energy occurs when the mechanism is in its undeflected position. This position is shown in solid lines in Fig. 7.7(a). The second stable equilibrium position has some energy stored but is a local minimum of potential energy and therefore is a stable equilibrium position. The energy stored is evident in the deflected member shown in dashed lines in Fig. 7.7(a).

7.2 Example Compliant Mechanism Research Areas

There are many active research topics in compliant mechanisms and new areas continue to be discovered. A subset of topics is mentioned here and then three examples are discussed in more depth. Compliant mechanism design methods have been an important area of research. This includes optimization methods [10, 11, 23, 27, 43, 45, 48, 50, 56], design of precision flexures [6, 16, 17, 31, 46, 54], building blocks [30], and the pseudo-rigid-body model approach discussed previously. Classes of compliant mechanisms studied include multistable mechanisms [4, 5, 28, 33, 41], metamorphic mechanisms [8, 9, 52], contact-aided compliant mechanisms [3, 13, 34, 35], compliant joints [40, 49, 55], medical devices [7, 36], origami inspired mechanisms [12] and statically balanced mechanisms [14, 42]. Analysis of nonlinear deflections [2, 15] and dynamics of compliant mechanisms [51, 53] are two of many analysis topics under study. Three examples of compliant mechanism research areas are provided next, including microelectromechanical systems (MEMS), biomedical implants, and lamina emergent mechanisms.

7.2.1 Microelectromechanical Systems (MEMS)

Compliant mechanisms[2] are well suited for application at the micro scale. The fact that they can be fabricated from a single layer makes them compatible with many

[2]This section is based on Compliant Mechanisms, by L.L. Howell in *Encyclopedia of Nanotechnology*, Editor: B. Bhusham, Springer, 2012, used with permission.

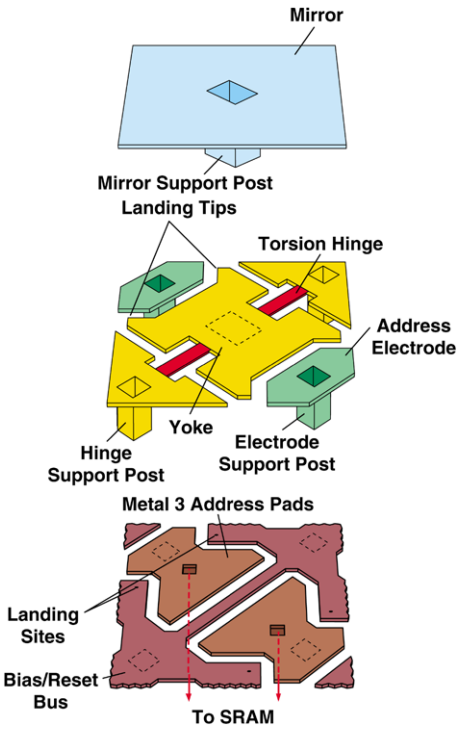

Fig. 7.8 Texas Instruments Digital Micromirror Device (DMD™) uses compliant torsion hinges to facilitate mirror motion. (Illustration courtesy of Texas Instruments)

MEMS fabrication methods. The elimination of assembly and friction is also important for micro devices. Examples of MEMS compliant mechanisms are shown here to illustrate their properties and to demonstrate a few applications.

Digital Micromirrors One of the most visible commercially available microelectromechanical systems is Texas Instruments Digital Micromirror Device (DMD™) which is used in applications such as portable projectors. The DMD is a rectangular array of moving micromirrors that is combined with a light source, optics, and electronics to project high quality color images. Figure 7.8 shows the architecture of a single DMD pixel. A 16 micrometer square aluminum mirror is rigidly attached to a platform (the "yoke"). Flexible torsion hinges are used to connect the yoke to rigid posts. An applied voltage creates an electrostatic force that causes the mirror to rotate about the torsion hinges. When tilted in the on position, the mirror directs light from the light source to the projection optics and the pixel appears bright. When the mirror is tilted in the off position, the light is directed away from the projection optics and the pixel appears dark. The micromirrors can be combined in an array on a chip, and each micromirror is associated with the pixel of a projected image. The torsion hinges use compliance to obtain motion while avoiding rubbing parts that cause friction and wear. The hinges can be deflected thousands of times per second and infinite fatigue life is essential.

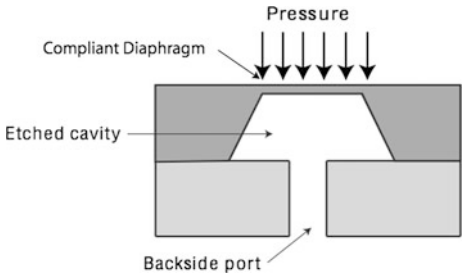

Fig. 7.9 The strain on a compliant diaphragm of a piezoresistive pressure sensors results in a detectable change in resistance, which is correlated with the pressure

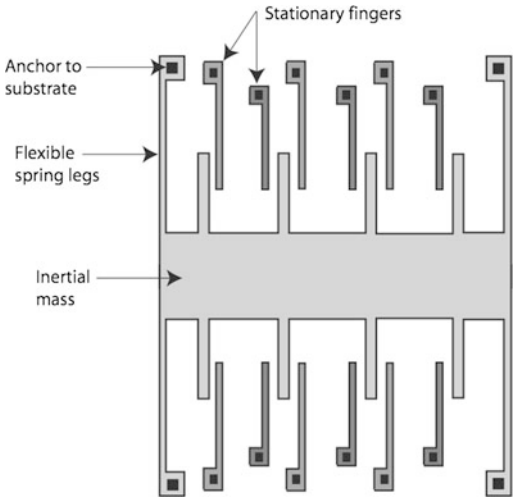

Fig. 7.10 This accelerometer makes use of compliant legs that deflect under inertial loads. The deflection results in a detectable change in capacitance and is correlated with the corresponding acceleration

Piezoresistive Pressure Sensors A sensor is a device that responds to a physical input (such as motion, radiation, heat, pressure, magnetic field), and transmits a resulting signal that is usually used for detection, measurement, or control. Advantages of MEMS sensors are their size and their ability to be more closely integrated with their associated electronics. Piezoresistive sensing methods are among the most commonly employed sensing methods in MEMS. Piezoresistance is the change in resistivity caused by mechanical stresses applied to a material. Bulk micromachined pressure sensors have been commercially available since the 1970s. A typical design is illustrated in Fig. 7.9. A cavity is etched to create a compliant diaphragm that deflects under pressure. Piezoresistive elements on the diaphragm change resistance as the pressure increases; this change in resistance is measured and is correlated with the corresponding pressure.

Capacitive Acceleration Sensors Accelerometers are another example of commercially successful MEMS sensors. Applications include automotive airbag safety systems, mobile electronics, hard drive protection, gaming, and others. Figure 7.10 illustrates an example of a surface micromachined capacitive accelerometer. Acceleration causes a displacement of the inertial mass connected to the compliant suspension, and the capacitance change between the comb fingers is detected.

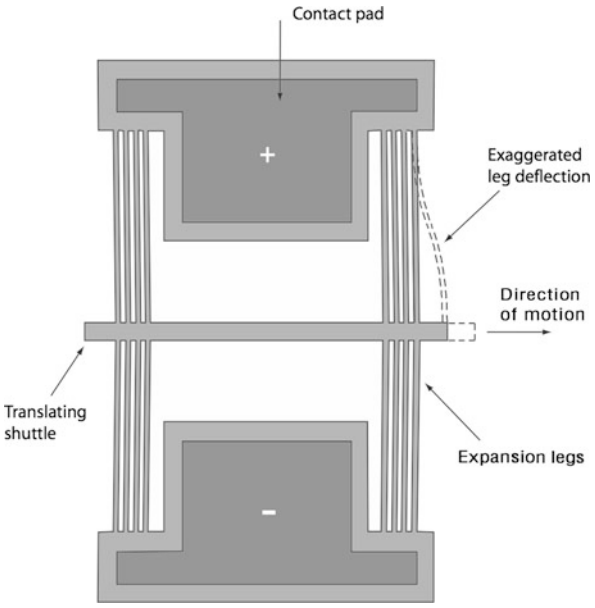

Fig. 7.11 A schematic of a thermomechanical in-plane microactuor (TIM) that uses compliant expansion legs to amplify the motion caused by thermal expansion

Thermal Actuators A change in temperature causes an object to undergo a change in length, where the change is proportional to the material coefficient of thermal expansion [22]. This length change is usually too small to be useful in most actuation purposes. Therefore, compliant mechanisms can be used to amplify the displacement of thermal actuators. Figure 7.11 illustrates an example of using compliant mechanisms to amplify thermal expansion in microactuators. Figure 7.12 shows a scanning electron micrograph of a Thermomechanical In-plane Microactuator (TIM) illustrated in Fig. 7.11. It consists of thin legs connecting both sides of a center shuttle. The leg ends not connected to the shuttle are anchored to bond pads on the substrate and are fabricated at a slight angle to bias motion in the desired direction. As voltage is applied across the bond pads, electric current flows through the thin legs. The legs have a small cross sectional area and thus have a high electrical resistance, which causes the legs to heat up as the current passes through them. The shuttle moves forward to accommodate the resulting thermal expansion. Advantages of this device include its ability to obtain high deflections and large forces, as well as its ability to provide a wide range of output forces by changing the number of legs in the design.

7.2.2 Biomedical Compliant Mechanisms

Compliant mechanisms are well suited for application in biomedical applications because of their low wear, the ability to be fabricated of biocompatible materials,

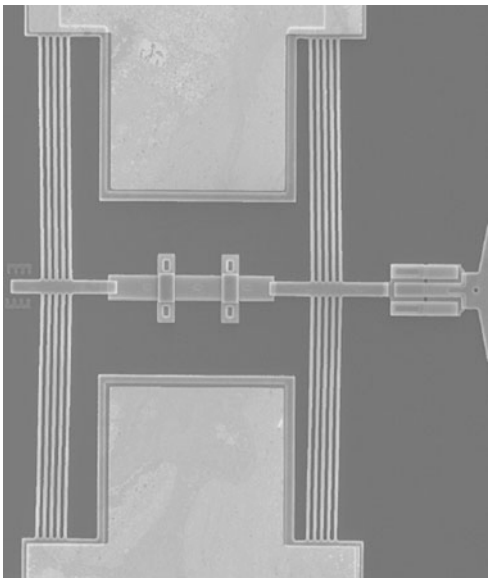

Fig. 7.12 A scanning electron micrograph of a thermal actuator illustrated in Fig. 7.11

and their compactness. There are many possible research areas and applications, and one implant is described here as a illustrative example.

The design objective of the spinal implant is to restore healthy physiologic biomechanics to the degenerated spinal segment. Because the healthy motion and the degree of mechanical dysfunction of the spine varies significantly from person to person [37, 39], the device is tailorable to the needs of the patient via surgeonselectable inserts. There may also be therapeutic benefits to intentional adjustment of the devices stiffness to induce and support remodeling of the surrounding tissue architecture [44]. This example discusses the design and validation of a spinal implant capable of nonlinear stiffness and adjustability, including analytical and numerical models, benchtop, and cadaveric testing results.

Example Implant Design A compliant mechanism[3] was designed as a spinal implant to share load with a damaged or diseased intervertebral spinal disc, as shown in Fig. 7.13.

The baseline configuration of the spinal implant is based on the lamina emergent torsional (LET) joint [47]. The LET geometry offers advantages in terms of manufacturability and independently controlled flexibility in multiple directions [24, 25]. The device consists of a LET joint that has been split into two parts that are independently attached to the vertebral pedicles. The vertebra themselves act as semirigid connections between the two parts of the LET joint. The attachment to the vertebral pedicles is accomplished via pedicle screws. Each half of the baseline device

[3]This section is based on "Spinal Implant Development, Modeling, and Testing to Achieve Customizable and Nonlinear Stiffness" by E. Dodgen, E. Stratton, A.E. Bowden, L.L. Howell, in *Journal of Medical Devices*, vol. 6, doi:10.1115/1.4006543, 2012. Used with kind permission © ASME.

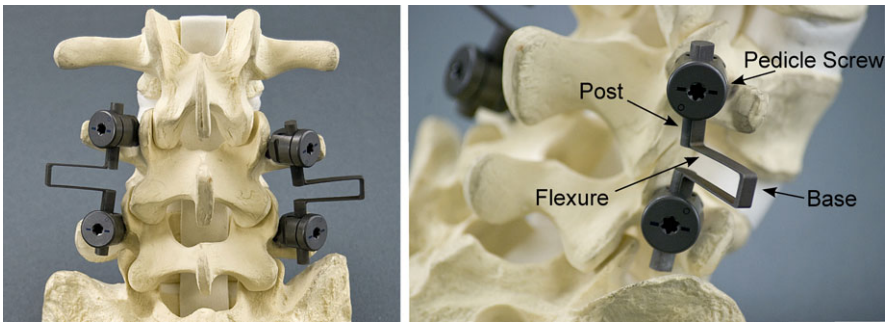

Fig. 7.13 Prototype of the baseline configuration

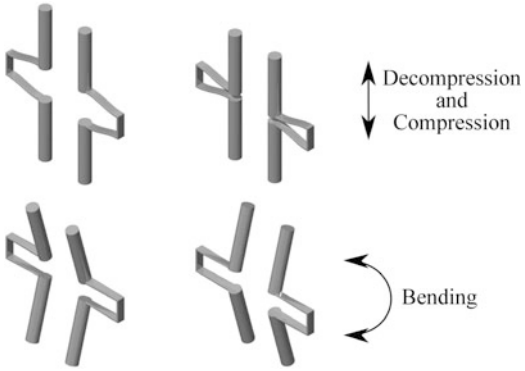

Fig. 7.14 Deflected positions of the baseline configuration

configuration is composed of two attachment posts, two flexures, and a central connecting beam. The two flexures and the central connecting beam form a C-shape. The bilateral components are positioned on either side of the two vertebral bodies to which they are attached. Optional inserts adjust the force-deflection response of the flexures to meet the target spinal kinetic response deemed appropriate for the individual patient. Figure 7.14 shows the baseline configuration deflected in the two modes of loading for which it was designed.

The optional contact-aided insert design is configured as two parts which connect together and attach to the central connecting beams of the baseline device. The elliptical contact surfaces of the inserts are designed such that as the flexures of the baseline configuration deflect during spinal motion, they come into contact with the surfaces, altering the force deflection relationship in a controlled and specific manner, as shown in Figs. 7.15 and 7.16.

Through alteration of the elliptical parameters for the contact surfaces, the insert can be modified to provide a wide range of variability in stiffness. The intended use is for clinicians to select the desired insert configurations appropriate to the patient pathology. If the response of the implant needs to be modified due to changes in the patient pathology, then the insert can be replaced without changes to the pedicular attachment sites. Figure 7.17 displays a prototype of the insert and how it attaches to

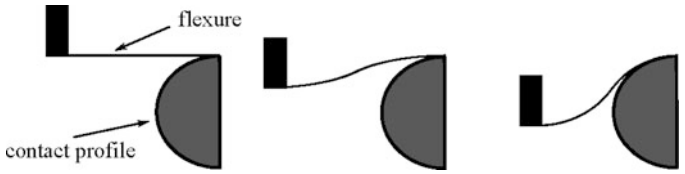

Fig. 7.15 Contact-aided flexure shown deflected on a circular contact profile

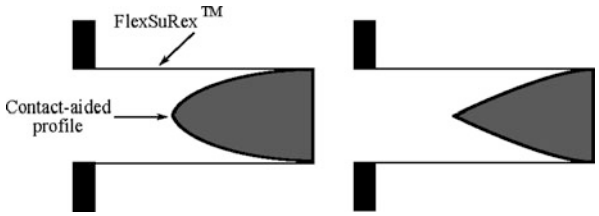

Fig. 7.16 Contact-aided flexure and two different contact profiles

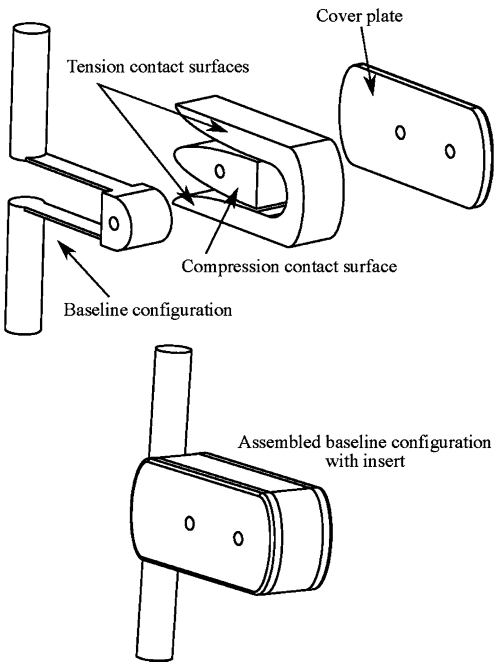

Fig. 7.17 Contact-aided attachment for baseline configuration

the baseline configuration of the implant. The dimensions of the baseline configuration and the semimajor a and semiminor b axes of the elliptic surfaces are shown in Fig. 7.18. The surfaces of the insert are positioned such that the flexures come into contact with them as the device is pulled in tension (i.e., during flexion and during contralateral bending) or compressed (i.e., during extension and during ipsi-

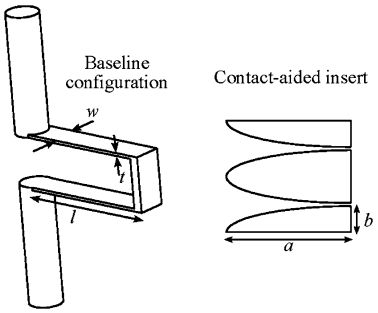

Fig. 7.18 Baseline configuration with contact surface dimensions defined

lateral bending). The elliptical geometry of the insert used in conjunction with the flexures geometry defines the stiffness of the implant. The ideal design performance of the device was evaluated using analytical modeling, finite element modeling, and benchtop testing of prototypes.

7.2.3 Lamina Emergent Mechanisms (LEMS)

Lamina emergent mechanisms (LEMs)[4] are mechanical devices fabricated from planar materials (laminae) with motion that emerges out of the fabrication plane. They achieve their motion from the deflection of flexible members (and are therefore compliant mechanisms [21]) and are monolithic within each planar layer. The attraction of LEMs lies in their potential to perform sophisticated mechanical tasks with simple topology. The ability to fabricate them from planar layers of material makes it possible to pursue manufacturing using simplified processes common to sheet materials. Thus, LEMs offer the potential for high performance, compact devices that can be fabricated at low manufacturing cost, but with the tradeoff of challenging design issues. The development of fundamental principles in LEMs has the potential to release a flood of new LEM applications [26]. Consider some generic examples of LEMs. Figure 7.19(a) shows a pantograph mechanism (a multidegree-of-freedom device used for scaling force or motion) and Fig. 7.19(b) shows a multistage mechanism. Plan views of the devices are shown on the left and prototypes on the right. Figure 7.20(a) is a scanning electron micrograph of a rigid-link, three-degrees-of-freedom micromechanism[32] that is fabricated using planar layers of material and has motion out of the plane. A compliant counterpart is shown in Fig. 7.20(b).

[4]This section is based on "Lamina Emergent Mechanisms and Their Basic Elements," by J.O. Jacobsen, B.G. Winder, L.L. Howell, and S.P. Magleby, *Journal of Mechanisms and Robotics*, vol. 2, No. 1, 011003-1 to 011003-9, 2010. Used with kind permission © ASME.

7.2.3.1 Advantages of LEMs

The interest in LEMs comes from the advantages inherent in their nature: being fabricated in a plane, having a flat initial state, and being monolithic. Each of these characteristics and its associated advantages are briefly described below.

Fabricated in a Plane The fact that LEMs can be fabricated from planar layers influences both what processes can be used for their manufacture and what materials may be used in their construction. The use of low-cost, high-quality sheet goods has the potential to dramatically reduce cost for high-volume production. At the microlevel, LEMS can be fabricated using single-layer MEMS fabrication methods and materials, which offers significant cost and reliability advantages. It also provides opportunities for complex out-of-plane motion with only a single layer.

At the macrolevel, manufacturing processes used to make static structures or components for assembly can be used to create mechanisms capable of sophisti-

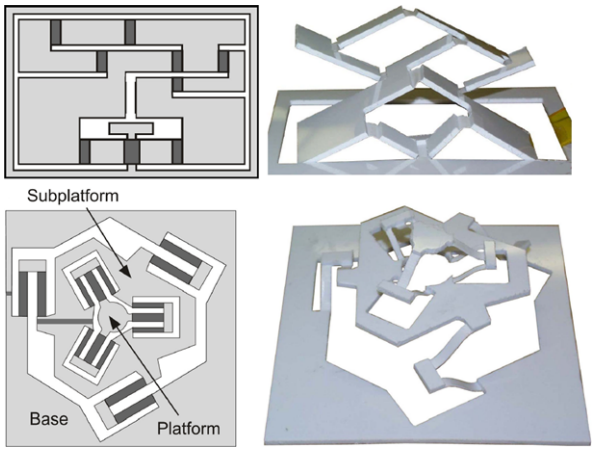

Fig. 7.19 Examples of LEMs, including (**a**) a pantograph mechanism, and (**b**) a multiple stage platform. In both (**a**) and (**b**) the darker sections in the schematics are flexible elements. The pictures on the right are polypropylene models

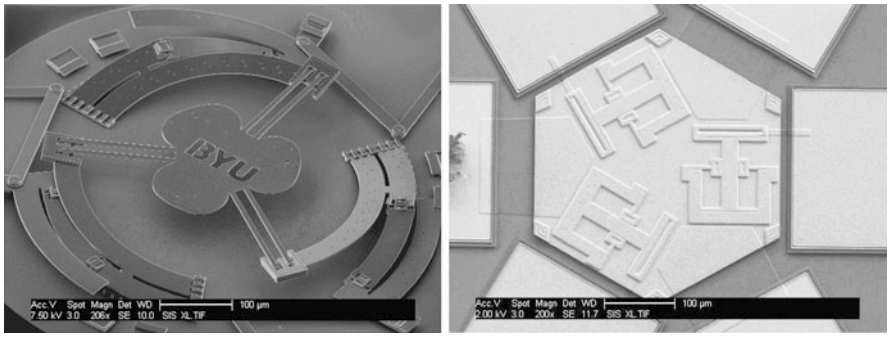

Fig. 7.20 Scanning electron micrographs (SEMs) of (**a**) a rigid-link three-degrees-of-freedom microplatform made using multiplelayers, and (**b**) a compliant counterpart

cated motions and complex tasks. Example processes include stamping, fine blanking, laser cutting, water jet cutting, plasma cutting, and wire electrical discharge machining (EDM). Some of these processes, such as stamping, offer significant cost advantages for high-volume production.

Flat Initial State The potential for many LEMs to have a flat initial state provides opportunities for extreme compactness. Compact mechanisms are particularly attractive in applications with highly constrained space. Another advantage is found in applications where it is important for the device to be compact during transport and then deployed when at its location of operation. An obvious advantage of a flat initial state is compact packaging and shipping, which can mean a significant reduction in the cost of handling, storing, and shipping high volumes of devices.

Not all LEMs will be flat after fabrication because some may be shaped using the same processes used to create the mechanism (e.g., stamping operations). There is also the possibility of using residual stresses in MEMS processes to move the after-fabricated position out of plane. But the nonflat mechanisms still have the characteristic of being monolithic, which is discussed next.

Monolithic The single-piece, or monolithic, nature of LEMs brings with it many of the characteristics of compliant mechanisms in general. The creation of controlled motion without pin joints provides opportunities for increased precision because of the elimination of backlash and wear. Weight can be reduced by using compliant mechanisms, and friction between rubbing parts can be reduced or eliminated. While multilayer LEMs require assembly, for monolithic devices, assembly of mechanism parts is often unnecessary.

7.2.3.2 Challenges of Lamina Emergent Mechanism Design

Taking advantage of the benefits of lamina emergent mechanisms often requires overcoming their inherent challenges. First, the desired motions are often too large to be modeled using linearized equations such as those commonly used in beam equations or linear finite element analysis. Thus, any successful modeling approach must be capable of addressing the intrinsic nonlinearities of the problem. Second, there are singularities inherent in LEM analysis because of the planar nature of the fabricated position. LEMs are change-point mechanisms in their fabricated state, and multiple motions are possible for a given input. Third, unlike those in rigid-body mechanisms, the motions in LEMs are highly coupled with stress, fatigue, and energy stored in a system.

By leveraging the unique performance and cost-saving characteristics possible with LEMs, many innovations become possible. Improvements can be made to existing products, and new products with unprecedented performance can be created. Products that were economically impractical with other technologies could become viable in a competitive marketplace with LEM technology.

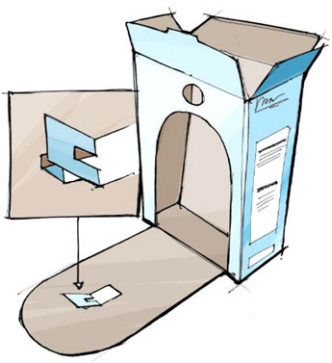

Fig. 7.21 Cereal boxes and other packaging could be used to create entertaining games for children

7.2.3.3 Potential Applications of LEMs

Various categories of opportunities[5] are enabled by combining the advantages of the different functional characteristics of LEMs. Descriptions of these opportunities are below.

Disposable Mechanisms By using low-cost, planar manufacturing techniques to create mechanisms with little or no assembly required, production of LEMs can be very inexpensive. Flat initial states can further reduce costs through compact shipping. Such low-cost mechanisms could be considered disposable.

There are many possible applications for disposable LEMs. Sterile products could use emerging packaging so that opening the packaging causes a motion to present the non-sterile end to the user for easy removal. Cereal boxes and other cardboard packaging could have LEMs that emerge into entertaining games for children (see Fig. 7.21).

Radio frequency identification is becoming more common in credit cards, allowing users to complete transactions more quickly and easily. However, this can also be a source for identity theft by scanning a card in someones pocket. A LEM could be used as a credit card Faraday cage to cover the chip until the device is deployed for use (see Fig. 7.22). Alternatively, the receiving or signaling circuits could remain open until the user actuates a LEM to make electrical contact during a credit card transaction. The low cost of these devices allows companies to continue mailing credit card offers that are often viewed as disposable.

Novel Arrays An array in this context is defined as a patterned arrangement, normally in rows and columns. LEMs that are composed of an array of mechanisms

[5]This section is based on "Identifying Potential Applications for Lamina Emergent Mechanisms Using Technology Push Product Development," by N.B. Albrechtsen, S.P. Magleby, and L.L. Howell, in *Proceedings of the ASME International Design Engineering Technical Conferences*, Montreal, Quebec, Aug. 15–18, 2010, DETC2010-28531, used with permission. Used with kind permission © ASME.

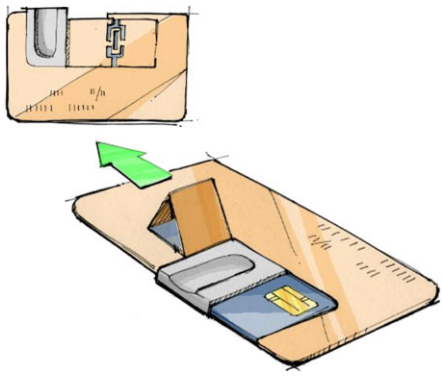

Fig. 7.22 A LEM used as a Faraday cage to cover the radio frequency identification chip on credit cards to prevent identity theft

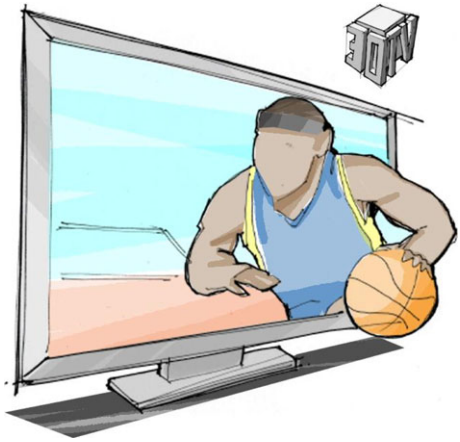

Fig. 7.23 A television where each pixel is a LEM, creating a moving, three-dimensional image

could benefit from all three functional characteristics. If a large array with many mechanisms required manual assembly, the labor costs associated with production might preclude that product from becoming economically viable. By using a stamping process, eliminating assembly through compliance, and transporting compactly in the flat initial state, price can be reduced significantly. LEMs may enable many novel arrays that were previously cost prohibitive.

LEMs that use arrays are perhaps the largest group of potential applications for the technology. A LEM printed circuit board could integrate a qwerty key-board with its underlying circuitry into a single piece device. A television screen in which each pixel could emerge from the viewing plane would create a more realistic three dimensional experience (see Fig. 7.23). A similar array could be used to give tactile responses to users in a virtual reality environment.

LEM arrays would experience widespread use if applied to electricity generation. Energy could be harvested from urban pedestrian traffic, wind, waves, or highway pavement compression.

Creating an array of small surfaces that can be oriented to face in different directions would be useful in many application areas. A guided LEM solar array would

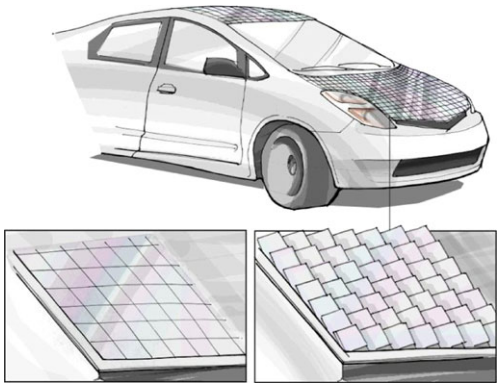

Fig. 7.24 A guided array of solar panels mounted on a vehicle

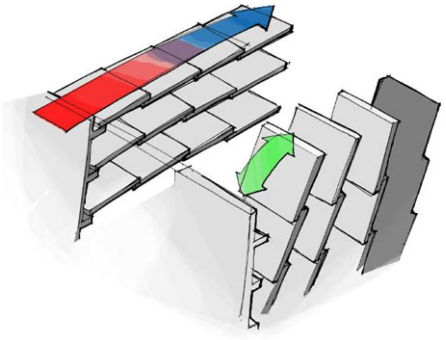

Fig. 7.25 Using LEMs, heat fins could be reconfigured into insulation, allowing a dynamic thermal resistance

dramatically reduce the bulk of current solar trackers, perhaps allowing them to be mounted on the surfaces of vehicles or buildings (see Fig. 7.24). A directional array could be used to reflect, combine, and diffract various media such as waves, signals, or light. A directional array could create dynamic acoustics, radar-diverting stealth surfaces, improved satellites, or artistic lighting effects. The mechanism would even have the ability provide a variable surface texture. This might be used to manipulate drag characteristics for guiding projectiles, create air resistance for rapid braking, or regulate flow rates in pipes. It could also be used to change the traction of contact surfaces.

LEM arrays could become powerful tools to influence thermal properties. By stacking layers of LEMs, a kinetic insulation could be possible. Deploying the mechanisms would increase the amount of air contained in the insulation, thereby increasing the thermal resistance. This is advantageous over existing kinetic insulations because it only requires a simple mechanical input instead of pressurization [38]. The layers of LEM insulation could even be reconfigured into heat fins, converting the device from a heat shield into a heat sink (see Fig. 7.25).

Deployable rebar structures are another application that could benefit from a pattern of co-planar joints. Current rebar structures require extensive manual assembly that consists of fastening rods together using wire and hand tools. Instead, large sections of rebar structures could be stamped and deployed into the desired config-

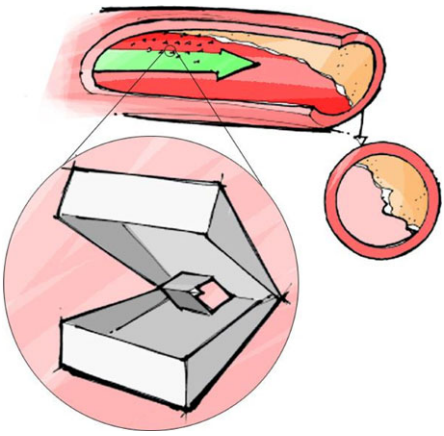

Fig. 7.26 Microscopic LEMs could be placed in the bloodstream to erode plaques from arteries

uration with one or two simple inputs. This could dramatically reduce labor costs and the duration of construction projects, which may be particularly important for rebuilding after a disaster.

Scaled Mechanisms The planar fabrication and potential to eliminate assembly through compliance allows for scaling to very small sizes. Using micromachining techniques, LEMs can be developed on the micro scale. In addition, mechanisms that have been developed at the micro level can be scaled to fit larger applications.

Autonomous micro LEM devices could perform various operations on individual cells. Cells could be physically manipulated, tested for various diseases, and individually medicated. A large number of micro cutting mechanisms in the bloodstream could erode plaques from arterial walls, avoiding the need for invasive stents or bypass surgery (see Fig. 7.26). Similar mechanisms could be used to clean industrial piping. The devices could be removed from the process flow with magnets in order to maintain production rates.

Surprising Motion LEMs can have complex, unusual, and non-intuitive motion. A flat initial state causes LEM designs to have a very simple topology, and compliance allows LEMs to be monolithic. Therefore, the complex motion emerging from a single sheet of material is often impressive to users.

The complex motion that springs from a simple LEM can surprise users and attract attention. This could be used in pop-up advertising that deploys when users open a products packaging for the first time. This could also create entertaining three dimensional board game layouts (see Fig. 7.27). Kits could be sold to help crafters create emerging images in scrap book pages. LEM business cards would increase interest and be memorable to potential customers.

Shock Absorbing The compliant nature of LEMs induces energy storage during motion. Not all of the energy is stored in LEMs. Some of the energy can be dissipated by conversion into heat and friction, giving LEMs an ability to dissipate energy as well.

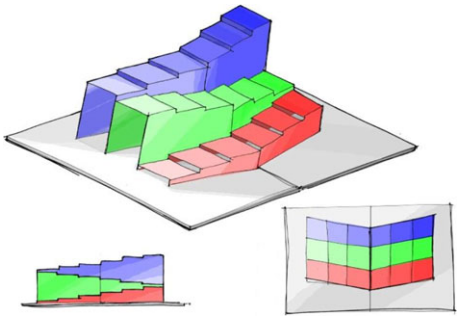

Fig. 7.27 A surprising three-dimensional board game made with a LEM

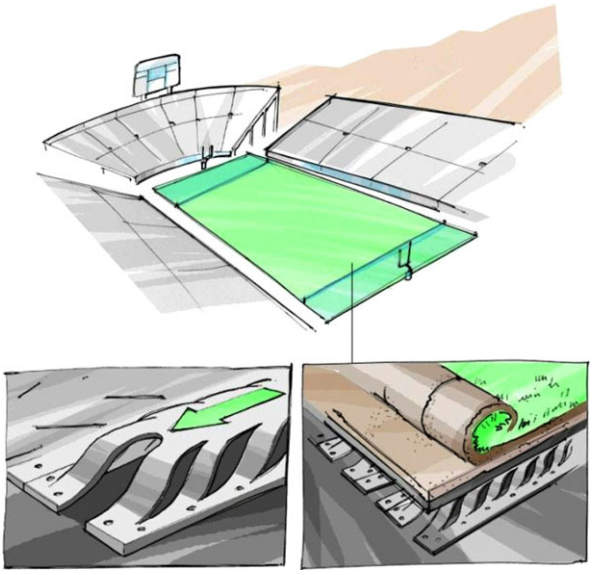

Fig. 7.28 Shock absorbing LEMs could allow better control over the spring and damping properties of athletic turf or flooring

The energy absorption of LEMs can be useful in many shock-absorbing products. Athletic flooring, turf, and footwear with a layer of energy absorbing LEMs could allow more control over the spring and damping properties than current padding (see Fig. 7.28).

This could reduce sports injuries that develop due to repeated impact. Protective armor could be manufactured with multiple layers of energy absorbing and dissipating LEMs, possibly improving upon current bullet-proof technologies [1]. A deploying spring system that encases sensitive electronics could cushion against drops that typically cause damage, and a flexible suspension matrix for crates of produce could also reduce bruising and cracking in the fruit and egg industries. Cushioning LEMs could be stamped into metal seating surfaces to allow a more comfortable distribution of body pressure.

Deployable Mechanisms LEMs can be transported in their flat initial state and then deployed onsite into an expanded configuration. This has the potential to dra-

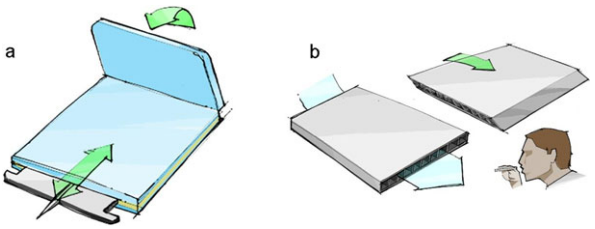

Fig. 7.29 Deployable mechanisms could be the size of a credit card to fit into a wallet for emergencies. Examples include (**a**) an adrenaline injector or (**b**) an inhaler

matically increase portability and decrease the cost of handling, storing, and shipping LEMs.

Mechanisms and structures with significant empty space are prime candidates to become deployable mechanisms. A deploying desk and chair could eliminate the need for an extra room for a home office, making them more available to the general population. International barge containers could be collapsed during return transport to reduce the cost associated with shipping empty space. Temporary structures could be LEMs, allowing innovative,deploying camping shelters, green houses, and field medical rooms.

Many deployable devices could be the size of a credit card and easily carried in a wallet for unexpected situations (see Fig. 7.29). A compact blood lancet for blood testing would be useful for diabetes patients. Credit card sized adrenaline injectors could be useful for people with serious allergies. A small inhaler could easily be carried by asthma patients for use in case of emergencies. Even a single-exposure, disposable camera could fit inside a wallet in case of unplanned photograph opportunities.

7.3 Conclusion

Compliant mechanisms provide significant benefits for motion applications. They can be compatible with many fabrication methods, may not require assembly, have friction-free and wear-free motion, provide high precision and high reliability, and they can integrate multiple functions into fewer components. The major challenges associated with compliant mechanisms come from the difficulty associated with their design, limited rotation, and the need to ensure adequate fatigue life. It is likely that compliant mechanisms will see increasing use in mechanical systems at all size scales and in many application domains as more people understand their advantages and have tools available for their development.

Acknowledgements This chapter is based on work done in collaboration with many other people, and the contributions of the co-authors on those works are gratefully acknowledged. This includes Spencer Magleby, Anton Bowden, Nathan Albrechtsen, Eric Dodgen, Eric Stratton, Joseph Jacobsen, and Brian Winder. The assistance of Danielle Peterson, Kevin Francis, Holly Greenberg and Larrin Wada are also appreciated. The author gratefully acknowledges support from Crocker Ventures, the Utah Technology Commercialization and Innovation Program, and the National Science Foundation through grant CMMI-0800606.

References

1. Andersen, C., Magleby, S., Howell, L.: Principles and preliminary concepts for compliant mechanically reactive armor. In: ASME/IFToMM International Conference on Reconfigurable Mechanisms and Robots (2009)
2. Awtar, S., Sen, S.: A generalized constraint model for two-dimensional beam flexures: nonlinear load-displacement formulation. J. Mech. Des. **132**(8)
3. Cannon, J.R., Howell, L.L.: A compliant contact-aided revolute joint. Mech. Mach. Theory **40**(11), 1273–1293 (2005)
4. Chen, G., Aten, Q.T., Zirbel, S., et al.: A tristable mechanism configuration employing orthogonal compliant mechanisms. J. Mech. Robot. **2**(1) (2010)
5. Chen, G., Gou, Y., Zhang, A.: Synthesis of compliant multistable mechanisms through use of a single bistable mechanism. J. Mech. Des. **133**(8) (2011)
6. Chen, S.-C., Culpepper, M.L.: Design of a six-axis micro-scale nanopositioner-hexflex. Precis. Eng. **30**(3), 314–324 (2006)
7. Cronin, J.A., Frecker, M.I., Mathew, A.S.: Design of a compliant endoscopic suturing instrument. J. Med. Dev. **2**(2) (2008)
8. Dai, J.S., Jones, J.R.: Matrix representation of topological changes in metamorphic mechanism. J. Mech. Des. **127**(4), 837–840 (2005)
9. Dai, J.S., Jones, J.R.: Mobility in metamorphic mechanisms of foldable/erectable kinds. J. Mech. Des. **121**(3), 375–382 (1999)
10. Frecker, M., Ananthasuresh, G., Nishiwaki, S., Kikuchi, N., Kota, S.: Topological synthesis of compliant mechanisms using multi-criteria optimization. J. Mech. Des. **11**(9), 238–245 (1997)
11. Frecker, M., Canfield, S.: Optimal design and experimental validation of compliant mechanical amplifiers for piezoceramic stack actuators. J. Intell. Mater. Syst. Struct. **11**(5), 360–369 (2000)
12. Greenberg, H.C., Gong, M.L., Howell, L.L., Magleby, S.P.: Origami and compliant mechanisms. J. Mech. Sci. **2**, 217–225 (2011)
13. Halverson, P.A., Howell, L.L., Magleby, S.P.: Tension-based multi-stable compliant rolling-contact elements. Mech. Mach. Theory **45**(2), 147–156 (2010)
14. Hoetmer, K., Woo, G., Kim, C., Herder, J.: Negative stiffness building blocks for statically balanced compliant mechanisms: design and testing. J. Mech. Robot. **2**(4) (2010)
15. Holst, G.L., Teichert, G.H., Jensen, B.D.: Modeling and experiments of buckling modes and deflection of fixed-guided beams in compliant mechanisms. J. Mech. Des. **133**(5) (2011)
16. Hopkins, J.B., Culpepper, M.L.: Synthesis of multi-degree of freedom, parallel flexure system concepts via freedom and constraint topology (FACT)—part I: Principles. Precis. Eng. **34**(2), 259–270 (2010)
17. Hopkins, J.B., Culpepper, M.L.: Synthesis of multi-degree of freedom, parallel flexure system concepts via freedom and constraint topology (FACT)—part II: Practice. Precis. Eng. **34**(2), 271–278 (2010)
18. Howell, L., DiBiasio, C., Cullinan, M., Panas, R., Culpepper, M.: A pseudo-rigid-body model for large deflections of fixed-clamped carbon nanotubes. J. Mech. Robot. **2**, 034501 (2010)
19. Howell, L., Midha, A.: Parametric deflection approximations for end-loaded, large-deflection beams in compliant mechanisms. J. Mech. Des. **117**, 156–165 (1995)
20. Howell, L., Midha, A.: A method for the design of compliant mechanisms with small-length flexural pivots. J. Mech. Des. **116**, 280–290 (1994)
21. Howell, L.L.: Compliant Mechanisms. Wiley, New York (2001)
22. Howell, L.L., McLain, T.W., Baker, M.S., Lott, C.D.: MEMS/NEMS Handbook, Techniques and Applications. Springer, New York (2006), pp. 187–200
23. Hull, P., Canfield, S.: Optimal synthesis of compliant mechanisms using subdivision and commercial FEA. J. Mech. Des. **128**(2), 337–348 (2006)
24. Jacobsen, J.O., Chen, G., Howell, L.L., Magleby, S.P.: Lamina emergent torsional (LET) joint. Mech. Mach. Theory **44**(11), 2098–2109 (2009)

25. Jacobsen, J.O., Howell, L.L., Magleby, S.P.: Lamina emergent mechanisms and their basic elements. J. Mech. Robot. **2**(1), 011003 (2010)
26. Jacobsen, J.O., Howell, L.L., Magleby, S.P.: Fundamental components for lamina emergent mechanisms. In: Proceedings of the 2007 ASME International Mechanical Engineering Congress and Exposition (2007)
27. Jain, C., Saxena, A.: An improved material-mask overlay strategy for topology optimization of structures and compliant mechanisms. J. Mech. Des. **132**(6) (2010)
28. Jensen, B.D., Howell, L.L.: Identification of compliant pseudo-rigid-body four-link mechanism configurations resulting in bistable behavior. J. Mech. Des. **125**(4), 701–708 (2003)
29. Jensen, B.D., Howell, L.L., Salmon, L.G.: Design of two-link, in-plane, bistable compliant micro-mechanisms. J. Mech. Des. **121**, 416–423 (1999)
30. Krishnan, G., Kim, C., Kota, S.: An intrinsic geometric framework for the building block synthesis of single point compliant mechanisms. J. Mech. Robot. **3**(1) (2011)
31. Lobontiu, N.: Compliant Mechanisms: Design of Flexure Hinges. CRC Press, Boca Raton (2003)
32. Lusk, C.P., Howell, L.L.: Components, building blocks, and demonstrations of spherical mechanisms in microelectromechanical systems. J. Mech. Des. **130**(3), 034503 (2008)
33. Lusk, C.P., Howell, L.L.: Spherical bistable micromechanism. J. Mech. Des. **130**, 1–6 (2008)
34. Mankame, N.D., Ananthasuresh, G.K.: Synthesis of contact-aided compliant mechanisms for non-smooth path generation. Int. J. Numer. Methods Eng. **69**(12), 2564–2605 (2007)
35. Mehta, V., Frecker, M., Lesieutre, G.A.: Stress relief in contact-aided compliant cellular mechanisms. J. Mech. Des. **131**(9), 091009 (2009)
36. Nai, T.Y., Herder, J.L., Tuijthof, G.J.M.: Steerable mechanical joint for high load transmission in minimally invasive instruments. J. Med. Dev. Trans. ASME **5**(3) (2011)
37. Natarajan, R.N., Andersson, G.B.J.: The influence of lumbar disc height and cross-sectional area on the mechanical response of the disc to physiologic loading. SPINE **24**(18), 1873–1881 (1999)
38. Nelson, P., Malecha, R., Chilenskas, A.: Variable pressure thermal insulating jacket (1994)
39. Panjabi, M.M., Goel, V., Oxland, T., Takata, K., Duranceau, J., Krag, M., Price, M.: Human lumbar vertebrae quantitative three-dimensional anatomy. SPINE **17**(3), 299–306 (1992)
40. Pei, X., Yu, J., Zong, G., Bi, S., Su, H.: The modeling of cartwheel flexural hinges. Mech. Mach. Theory **44**, 1900–1909 (2009)
41. Qiu, J., Lang, J.H., Slocum, A.H.: A curved-beam bistable mechanism. J. Microelectromech. Syst. **13**(2), 137–146 (2004)
42. Radaelli, G., Gallego, J.A., Herder, J.L.: An energy approach to static balancing of systems with torsion stiffness. J. Mech. Des. **133**(9) (2011)
43. Saxena, A., Ananthasuresh, G.K.: On an optimal property of compliant topologies. Struct. Optim. **19**(1), 3649 (2000)
44. Schnake, K.J., Putzier, M., Haas, N.P., Kandziora, F.: Mechanical concepts for disc regeneration. Eur. Spine J. **15**(Suppl. 3), 354–360 (2006)
45. Sigmund, O.: On the design of compliant mechanisms using topology optimization. Mech. Based Des. Struct. Mach. **25**(4), 493–524 (1997)
46. Smith, S.: Flexures: Elements of Elastic Mechanisms. Taylor, Francis, London (2000)
47. Stratton, E., Howell, L.L., Bowden, A.E.: Force-displacement model of the flexsure spinal implant (2010)
48. Sundaram, M.M., Limaye, P., Ananthasuresh, G.K.: Design of conjugate, conjoined shapes and tilings using topology optimization. Struct. Multidiscip. Optim. **45**(1), 65–81 (2012)
49. Trease, B.P., Moon, Y.-M., Kota, S.: Design of large-displacement compliant joints. J. Mech. Des. **127**, 788–798 (2005)
50. Wang, M.Y.: A kinetoelastic formulation of compliant mechanism optimization. J. Mech. Robot. **1**(2) (2009)
51. Wang, W., Yu, Y.: New approach to the dynamic modeling of compliant mechanisms. J. Mech. Robot. **2**(2) (2010)

52. Wuxiang, Z., Xilun, D.: A method for designing metamorphic mechanisms and its application (2009)
53. Yu, Y.Q., Howell, L.L., Lusk, C.P.: Dynamic modeling of compliant mechanisms based on the pseudo-rigid-body model. J. Mech. Des. **127**(4), 760–765 (2005)
54. Zhao, H., Bi, S., Yu, J.: A novel compliant linear-motion mechanism based on parasitic motion compensation. Mech. Mach. Theory **50**, 15–28 (2012)
55. Zhao, H., Bi, S., Yu, J.: Nonlinear deformation behavior of a beam-based flexural pivot with monolithic arrangement. Precis. Eng. **35**, 369–382 (2011)
56. Zhou, H., Killekar, P.: The modified quadrilateral discretization model for the topology optimization of compliant mechanisms. J. Mech. Des. **133**(11) (2011)

Sposoby zwiększania wydajności druku 3D w metodzie FFF

Ways to increasing performance of FFF 3D printing method

ADAM ŁYŻWA *

DOI: 10.17814/mechanik.2016.12.543

W artykule przedstawiono trzy metody zwiększania wydajności druku 3D metodą FFF. Próby polegały na zwiększaniu gęstości wypełnienia, wysokości warstwy oraz prędkości druku. Na podstawie wydruków testowych oraz symulacji porównano czasy, zużycie materiału oraz jakość wykonanego przedmiotu przy założonych parametrach druku.
SŁOWA KLUCZOWE: druk 3D, metoda FFF, wydajność druku 3D

Abstract: This article presents three methods of improving efficiency of 3D printing by the FFF method. Trials consisted of increasing the density of infill, layer height and print speed. On the basis of test prints and simulations, made with assumed parameters of printing, times, material consumption and quality wear compared.
KEYWORDS: 3D printing, method FFF method, efficiency of 3D printing

Metoda FFF (ang. *Fused Filament Fabrication*) [1] jest popularną metodą druku 3D, stosowaną w firmach produkcyjnych, biurach projektowych oraz w małych firmach i domach. Wraz ze wzrostem zapotrzebowania na elementy powstające w technologiach przyrostowych, zwiększają się wymogi odnośnie do wydajności procesu ich powstawania. Jako główne czynniki wpływające na efektywność procesu druku 3D przyjęto czas wykonania detalu oraz ilość zużytego materiału. Oba te parametry przekładają się bezpośrednio na koszty wytworzenia elementów. Badaniom poddano zmianę wydajności procesu w zależności od gęstości wypełnienia wydruku, wysokości drukowanej warstwy oraz prędkości drukowania. Jako dodatkowy parametr wzięto pod uwagę jakość wykonanych detali. Wszystkie próbki wydrukowano na urządzeniu GATE 3D firmy 3Novatica [2], z tworzywa PLA [3]. G-kody zostały wygenerowane w programie Cura w wersji 15.02.1. Program sterujący drukarką to Pronterface w wersji 2014.08.01. Przeprowadzone próby pokazały, jak różne wartości testowanych parametrów wpływają na zmianę czasu powstawania wydruków oraz na zużycie materiału. Na podstawie próbnych wydruków pokazano, jaki wpływ mają różne wartości poszczególnych parametry na jakość uzyskanych przedmiotów.

Zmniejszenie gęstości wypełnienia wydruku

W procesie przygotowania modelu do druku można regulować gęstości wypełnienia wnętrza elementu. Gęstość ustawia się w zakresie od 0% – obiekt pusty w środku (skorupa), do 100% – obiekt lity. Niektóre programy dają możliwość używania różnych wzorów wypełnienia. Rodzaj wypełnienia nie ma znaczącego wpływu na wydajność procesu. Najczęściej stosowanym wypełnieniem jest kratka.

Zestawienie czasów oraz zużycia materiałów dla różnych gęstości wypełnienia przedstawiono graficzne na rys. 1. Próbkę wydrukowaną przy wypełnieniu 0% pokazano na rys. 2.

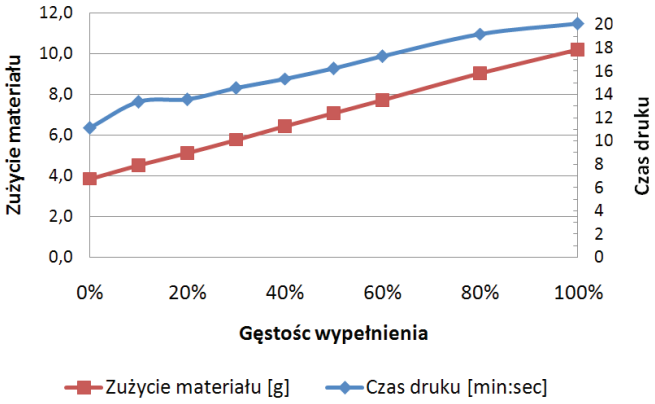

Rys. 1. Czas druku oraz zużycie materiału przy różnej gęstości wypełnienia

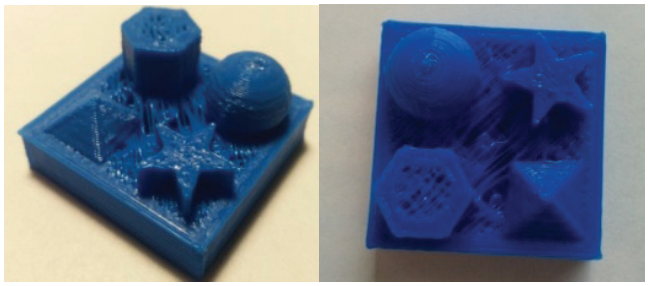

Rys. 2. Model wydrukowany przy wypełnieniu 0% (źródło własne)

Zwiększanie wysokości warstwy

Inną metodą na poprawę wydajności druku jest zwiększenie wysokości pojedynczej warstwy wydruku. Zakres grubości warstwy dla większości drukarek działających w technologii FFF to 0,06–0,3 mm. Zestawienie czasów oraz zużycia materiału dla różnych wysokości drukowanej warstwy przedstawiono graficznie na rys. 3. Jakość powierzchni drukowanych przedmiotów przedstawiono na rys. 4–6.

* Mgr inż. Adam Łyżwa (adam.lyzwa@dokt.p.lodz.pl) – Politechnika Łódzka, Wydział Mechaniczny, Instytut Obrabiarek i Technologii Budowy Maszyn

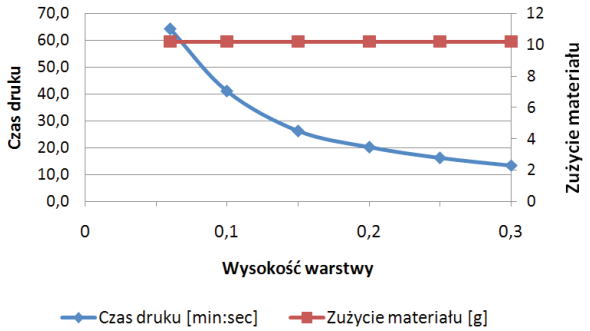

Rys 3. Czas druku oraz zużycie materiału dla różnej wysokości pojedynczej warstwy

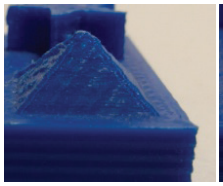

Rys. 4. Wysokość warstwy: 0,06 mm (źródło własne)

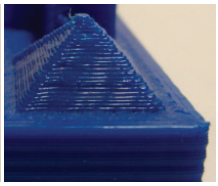

Rys. 5. Wysokość warstwy: 0,2 mm (źródło własne)

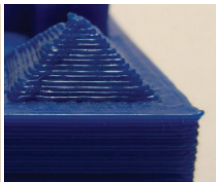

Rys. 6. Wysokość warstwy: 0,3 mm (źródło własne)

Zwiększenie prędkości druku

W procesie generowania kodu istnieje możliwość zmiany kilku różnych parametrów związanych z prędkością, tj. prędkość druku – ogólna prędkość poruszania się głowicy podczas druku, prędkość druku pierwszej warstwy, prędkość druku wypełnienia, prędkość druku ścian zewnętrznych, prędkość druku ścian wewnętrznych. W celu określenia zmian wydajności druku, wszystkie parametry prędkości zostały ustawione na tę samą wartość. Wyniki symulacji przedstawiono na rys. 7. Wydrukowane próbki przedstawiono na rys. 8–10.

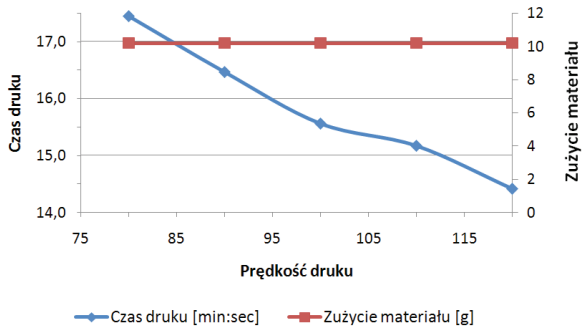

Rys. 7. Czas druku oraz zużycie materiału dla różnej prędkości druku

Rys. 8. Prędkość druku: 80 mm/s (źródło własne)

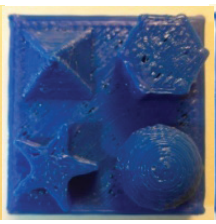

Rys.. 9. Prędkość druku: 100 mm/s (źródło własne)

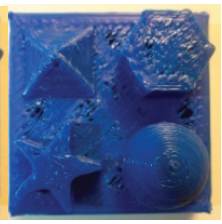

Rys. 10. Prędkość druku: 120 mm/s (źródło własne)

Podsumowanie

Wszystkie przedstawione w artykule metody modyfikacji parametrów druku są w stanie wpłynąć na polepszenie wydajności procesu wytwarzania metodą FFF. Niektóre z przedstawionych metod powodują wzrost wydajności zarówno czasowej, jak i materiałowej, inne natomiast skracają tylko czas wydruku.

Metoda zmiany gęstości wypełnienia pozwala zarówno skrócić czas wydruku, jak i zredukować ilość zużytego materiału (rys. 1). Próbne wydruki pokazały, że stosowanie wypełnienia o wartości 0% może powodować znaczny spadek jakości wykonanego elementu (rys. 2). Decydując się na wydruk pusty w środku, należy zwrócić uwagę na jego kształt i przeznaczenie. Powierzchnie równoległe do powierzchni stołu drukarki będą bardzo zniekształcone i najprawdopodobniej poprzerywane.

Metoda zwiększania wysokości warstwy drukowanego elementu wpływa tylko i wyłącznie na skrócenie czasu wydruku (rys. 3). Zmiany te są bardzo znaczące. Wysokość pojedynczej warstwy ma również duży wpływ na jakość wytwarzanych przedmiotów. Wydruki o niskiej warstwie są bardziej dokładne i szczegółowe. Te drukowane warstwami o dużej wysokości mają widoczną prążkowaną strukturę ścian bocznych, natomiast elementy okrągłe i pochylone pod kątem są zniekształcone (rys. 4–6).

Metoda zwiększania prędkości druku daje możliwość skrócenia czasu wytwarzania detalu. Próby pokazały, że wraz ze wzrostem prędkości spada jakość wytwarzanych elementów. Przy wyższych prędkościach możemy zaobserwować zniekształcenia geometrii detalu – zaokrąglone i skręcone naroża oraz brak ciągłości powierzchni (rys. 8–10). W najgorszym przypadku przedmiot drukowany zbyt szybko może niedostatecznie przywierać do powierzchni stołu, co może spowodować podwijanie się krawędzi bocznych lub zerwanie go ze stołu w trakcie drukowania. Innym niebezpieczeństwem druku przy dużych prędkościach jest możliwość zgubienia kroku przez jeden z silników. Powoduje to przesunięcie się części detalu w osi *x* lub *y*.

W celu poprawy wydajności, a zarazem utrzymania dobrej jakości wytwarzanych modeli, należy mieszać ze sobą przedstawione w artykule metody. Należy przy tym brać pod uwagę przeznaczenie konkretnego elementu. Wydruki, w których strona wizualna nie odgrywa kluczowej roli, można drukować na podwyższonych parametrach prędkości oraz wysokości warstwy. Spowoduje to znaczne skrócenie czasu druku. Przedmioty, które służą celom pokazowym, należy wykonać przy niższych prędkościach i mniejszych wysokościach warstwy, co pozwoli uzyskać najlepszą jakość powierzchni i dobre odwzorowanie szczegółów. Zmniejszenie gęstości wypełnienia przedmiotów o dużych gabarytach pozwoli zredukować ilość potrzebnego materiału. Należy jednak pamiętać, że może to negatywnie wpłynąć na jakość ich powierzchni górnych. Na podstawie analizy próbnych wydruków oraz symulacji czasów i zużycia materiału można stwierdzić, że dla wypełnienia 20%, wysokości warstwy 0,1 mm oraz prędkości druku 80 mm/s, powinniśmy otrzymać dobry jakościowo przedmiot przy możliwie najkrótszym czasie wydruku oraz możliwie najmniejszym zużyciu materiału.

LITERATURA

1. http://www.stratasys.com/3d-printers/technologies/fdm-technology
2. http://3novatica.com/pl/
3. http://reprap.org/wiki/PLA
4. Czerwiński K., Czerwiński M. *„Drukowanie w 3D”*. INFOAUDIT Warszawa 2015. ISBN: 978-83-922674-3-0.
5. *„Leksykon naukowo-techniczny z suplementem”*. T. P-Ż. Warszawa: WNT, 1989, s. 1104, 1153. ISBN 83-204-0969-1.